THE ROLE OF THE N-END RULE PATHWAY IN CARDIOVASCULAR DEVELOPMENT, SIGNALING, AND HOMEOSTASIS

by

Dong Eun Kim

Bachelor of Science, Seoul National University, 2003

Master of Science, Seoul National University, 2006

Submitted to the Graduate Faculty of

the School of Pharmacy in partial fulfillment

of the requirements for the degree of

Master of Arts

UNIVERSITY OF PITTSBURGH

SCHOOL OF PHARMACY

This thesis was presented

by

Dong Eun Kim

It was defended on

October 6, 2010

and approved by

Song Li, MD. PhD., Associate Professor, Pharmaceutical Sciences

Regis R. Vollmer, PhD., Professor, Pharmaceutical Sciences

Yong J. Lee, PhD., Professor, Pharmacology and Chemical Biology

Jeffrey S. Isenberg, MD. MPH, Associate Professor, Pulmonary, Allergy, and Critical Care Medicine

Thesis Director: Yong Tae Kwon, PhD., Associate Professor, Pharmaceutical Sciences

THE ROLE OF THE N-END RULE PATHWAY IN CARDIOVASCULAR DEVELOPMENT, SIGNALING, AND HOMEOSTASIS

Dong Eun Kim, M.S.

University of Pittsburgh, 2010

ABSTRACT

The N-end rule pathway relates the *in vivo* half-life of a protein to the identity of its N-terminal residue. The conjugation of arginine (Arg) from Arg-tRNA^{Arg} to N-terminal Asp, Glu, or Cys is a universal eukaryotic protein modification that can lead to ubiquitylation and proteasomal degradation of the resulting Arg-conjugated proteins through the N-end rule pathway. The mammalian *ATE1* gene encodes Arg-transferase that mediates all known N-terminal arginylation reactions. *ATE1*$^{-/-}$ embryos die owing to various cardiovascular defects including ventricular hypoplasia, ventricular septal defect, and late angiogenesis. The genomewide functional proteomics previously identified a set of RGS proteins (RGS4, RGS5, and RGS16) as *in vivo* substrates of ATE1. These RGS proteins are important negative regulators of Gαq-activated signaling for myocardial growth and vascular maturation/integrity. In my first project, I attempted to determine the role of ATE1-dependent posttranslational arginylation in Gαq-dependent cardiac signaling. I constructed and characterized ATE1$^{-/-}$Gαq^{Tg} compound mutant mice, where Gαq is exclusively overexpressed in the heart from αMHC promoter. I found that while Gαq overexpression in the heart rescues significantly cardiac defects in ATE1-/- embryonic hearts, it does not cause a noticeable change in vascular defects. These results together suggest that ATE1 controls cardiac development and signaling in part through Gq-activated signaling pathways. In the second project, I generated RGS5 transgenic mouse (TG) strains overexpressing either MC-RGS5 (wild-type, short-lived) or MV-RGS5 (mutant, long-lived) from vascular smooth muscle-specific SM22α promoter to determine the physiological importance of RGS5 proteolysis in Gq signaling of VSMC. Both MC-RGS5 and MV-RGS5 mice were viable and fertile without any visible defects. However, MC-RGS5 female

mice demonstrated impaired delivery in that newborn pups were often found dead associated with an absence of milk in their stomachs. In contrast, MV-RGS5 mice did not show this phenotype. The mis-regulated RGS5 proteolysis in MC-RGS5 mice may result in the failure in oxytocin-induced uterine and mammary gland smooth muscle contraction. In summary, my research provides an insight into the role of N-end rule pathway in cardiovascular Gq signaling.

TABLE OF CONTENTS

LIST OF TABLES

LIST OF FIGURES

Chapter 1.

Chapter 2.

Chapter 3.

PREFACE

Dedicated to my family whom I love more than anyone else in the world

1.0 THE MAMMALIAN N-END RULE PATHWAY

Ubiquitin (Ub) is a highly-conserved small protein which is only 76 amino acids, whose conjugation to other proteins provides a signal for the proteasomal degradation by labeling proteins (Hershko and Ciechanover 1998; Sriram, Banerjee et al. 2009). The ubiquitin (Ub) system is composed of three enzymes (**Figure 1**). E1 Ub-activating enzyme activates ubiquitin by forming a thioester linkage between the cysteine sulfhydryl group of E1 enzyme and the C-terminal carboxyl group of ubiquitin. This activating process requires ATP as an energy source. The activated ubiquitin is transferred to a cysteine residue of E2 Ub-conjugating enzyme via trans-esterification reaction. In the last step, E3 Ub ligase enzyme recognizes the substrate protein and interacts with both E2 and substrate. The E3 enzyme creates an amide isopeptide bond between a lysine of the substrate protein and C-terminal of ubiquitin.

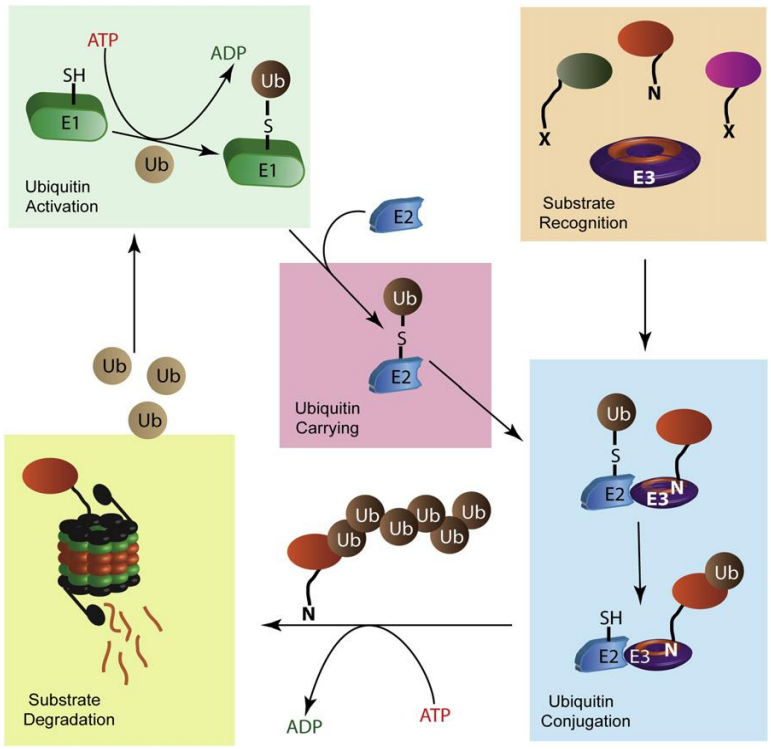

Figure 1. The ubiquitin system A protein substrate is conjugated to Ub through the E1-E2-E3 enzymatic cascade (Sriram, Banerjee et al. 2009).

The N-end rule pathway is a Ub-dependent protein degradation system where a class of E3s called *N-recognins* recognize type 1 (basic) and type 2 (bulky hydrophobic) destabilizing N-terminal residues of short-lived proteins as an essential determinant of N-terminal degradation signals called *N-degron* (Tasaki and Kwon 2007). N-terminal degradation determinants of the N-end rule pathway are divided into type 1 (basic; Arg, Lys, and His) and type 2 (bulky hydrophobic; Phe, Tyr, Trp, Leu, and Ile) destabilizing residues. An N-degron can be created by N-terminal modifications of a pre-N-degron. Since 1994, studies have identified approximately 10 genes involved in this process and characterized their gene products with respect to the conversion of pre-N-degron to N-degron (**Figure 2**).

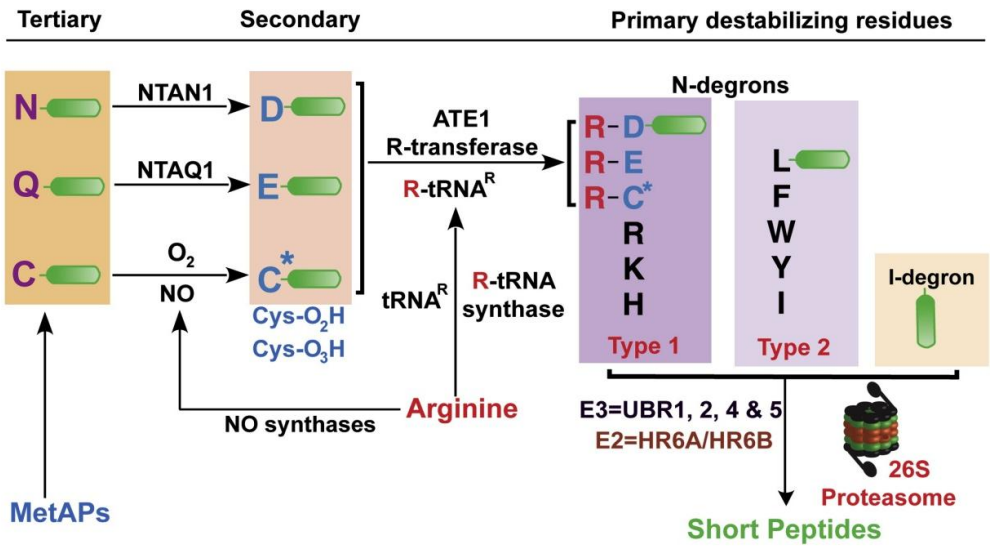

Figure 2. The hierarchical structure of the mammalian N-end rule pathway (Sriram, Banerjee et al. 2009).

One way to create destabilizing N-degron is through the removal of the N-terminal Met by Met aminopeptidases (MetAPs), which exposes the second residue at the N-terminus. Another way to create an N-degron is through endoproteolytic cleavage of a long-lived polypeptide, yielding a short-lived C-terminal fragment of the protein which consequently bears a destabilizing N-terminal residue. Intracellular endopeptidases can create a C-terminal fragment bearing a tertiary or secondary destabilizing residue or a primary destabilizing residue (de Groot, Rumenapf et al. 1991; Rao, Uhlmann et al. 2001; Ditzel, Wilson et al. 2003; Tasaki, Mulder et al. 2005; Tasaki and Kwon 2007). Specifically, exposed N-terminal Asn and Gln are tertiary destabilizing residues that function through their deamidation by N-terminal amidohydrolases (Nt-amidases), NTAN1 and NTAQ1, into the secondary destabilizing N-terminal residues Asp and Glu, respectively. Considering that knockout of NTAN1 selectively abolished the deamidation activity for N-terminal Asn, the hypothetical enzyme, termed NTAQ1, might be responsible for deamidation of N-terminal Gln, which remains unknown (Stewart, Arfin et al.

1995; Grigoryev, Stewart et al. 1996; Balogh, Kwon et al. 2000). NTAN1-deficient mice were shown to have defects in spontaneous activity, spatial memory and a socially conditioned exploratory behavior (Kwon, Balogh et al. 2000). N-terminal Asp and Glu are secondary destabilizing residues that function through their arginylation by ATE1-encoded Arg-tRNA-protein transferase (R-transferase), which creates the primary destabilizing residue Arg at the N-terminus. ATE1 encodes at least six isoforms and they exhibit differential cellular localization, tissue distribution and enzymatic activities for N-terminal Asp, Glu and Cys (Kwon, Kashina et al. 1999; Rai and Kashina 2005; Hu, Brower et al. 2006). Blunted arginylation activities of all known N-end rule substrates in ATE1-knockout mice suggested that ATE1 is the only enzyme responsible for N-terminal arginylation (Kwon, Kashina et al. 2002). ATE1-/- mouse embryos die at midgestation during embryogenesis primarily due to defects in cardiac development and angiogenesis (Kwon, Kashina et al. 2002). N-terminal Cys can also function as a tertiary destabilizing residue through its oxidation in a manner depending on nitric oxide (NO) and oxygen (O_2) or its derivatives; the oxidized Cys residue into Cys-sulfinic acid [$CysO_2(H)$] or Cys-sulfonic acid [$CysO_3(H)$] is subsequently arginylated by ATE1 (Kwon, Kashina et al. 2002; Hu, Sheng et al. 2005; Lee, Tasaki et al. 2005). Cys-sulfinic acid is structurally similar to Asp, one of known arginylation-permissive N-terminal residues, suggesting that the oxidation of N-terminal Cys is a specific modification to create a secondary destabilizing residue. The resulting N-terminal Arg together with other type 1 and type 2 N-degrons are recognized by N-recognins for protein ubiquitylation. Polyubiquitylated substrate with repeated conjugation of Ub is recognized and degraded by the proteolytic machinery of the ubiquitin-proteasome system (UPS), the 26S proteasome (**Figure 2**). Proteomic purification of endogenous E3s that bind to synthetic degrons, recently revealed a novel Ub ligase family, termed UBR1 through UBR7,

characterized by a ~70-residue domain, termed UBR box, that functions as a general substrate recognition domain (Tasaki, Mulder et al. 2005). Amongst these E3s, UBR1, UBR2, UBR4 and UBR5 were determined to have the ability to recognize N-degrons (Tasaki, Mulder et al. 2005). UBR box proteins have generally heterogeneous size and sequence but contain specific signatures as E3 Ub ligases or a substrate recognition subunit of the E3 complex: the RING domain in UBR1, UBR2 and UBR3; the HECT domain in UBR5; the F-box in UBR6 and the plant homeodomain (PHD) finger in UBR7. Characterization of knockout mice indicated that mammalian UBR1 and UBR2 are functionally overlapping N-recognins whose biochemical properties are similar to each other (Kwon, Reiss et al. 1998; Kwon, Levy et al. 1999; Kwon, Xia et al. 2001). UBR1-deficient mice develop Johanson-Blizard syndrome (JBS)-like phenotypes, including exocrine pancreatic abnormality, hypoglycemia and altered fat metabolism (Kwon, Xia et al. 2001). UBR2-deficient mice exhibit male-specific infertility and female-specific lethality that are distinguished from UBR1 null mice (Kwon, Xia et al. 2003). Mouse embryos lacking both UBR1 and UBR2, which share 46% of similarity, die at midgestation from impaired neurogenesis during development, indicating a functional interaction between these two E3s. UBR3-deficient neonatal pups die associated with impaired olfactory system, and UBR3 is prominently expressed in sensory cells for the five major senses (smell, touch, vision, hearing and taste), suggesting that UBR3 controls a general circuit underlying different sensory nervous systems. UBR4 with a size of 570 kDa binds to both type 1 and type 2 residues, interacts with human paillomavirus type 16 (HPV-16) E7 oncoprotein and retinobalastoma tumor suppressor protein (pRb) and has a role in anchorage-independent growth and cellular transformation in cancer cells (DeMasi, Huh et al. 2005; Huh, DeMasi et al. 2005). UBR5 (also known as EDD) with a size of 300 kDa, which preferentially bind to type 1 N-degron, has been implicated in

progesterone-regulated cell proliferation, DNA damage responses and tumorigenesis (Callaghan, Russell et al. 1998; Henderson, Munoz et al. 2006). The biochemical properties of UBR6 and UBR7 as N-recognins remain unclear.

2.0 POSTTRANSLATIONAL ARGINYLATION IN Gq-DEPENDENT CARDIAC DEVELOPMENT

2.1 OVERVIEW

The goal of this study is to determine the role of ATE1-dependent posttranslational arginaylation in Gαq-dependent cardiac signaling. The mammalian ATE1 gene-encoded Arg-transferase mediates all known N-terminal arginylation reactions (Kwon, Kashina et al. 2002). $ATE1^{-/-}$ embryos die owing to various cardiovascular defects including ventricular hypoplasia, ventricular septal defect (VSD), and late angiogenesis (Kwon, Kashina et al. 2002). These severe cardiovascular phenotypes are mainly due to the impaired proliferation of myocardium, especially cardiomyocytes where ATE1 is supposed to be prominently expressed, which precedes developmental defects observed during embryogenesis. The genomewide functional proteomics identified a set of RGS (Regulators of G-protein Signaling) proteins, RGS4, RGS5 and RGS16, as *in vivo* substrates of N-end rule that may underlie ATE1-dependent cardiovascular homeostasis (Lee, Tasaki et al. 2005). RGS4, RG55 and RGS16 have been known as important negative regulators of the Gq-activated signaling for myocardial growth and

vascular maturation/integrity. RGS4, known to regulate Gq-activated signaling, was found to be accumulated throughout the entire body of embryos lacking ATE1 (Lee, Kwon et al. unpublished). It has been found that Gq-activated signaling components, including protein kinase C (PKC) and its downstream component, MEK1 are downregulated in ATE1-deficient hearts (Lee, Kwon et al. unpublished). There results suggest that developmental defects in $ATE1^{-/-}$ hearts may be at least in part caused by dampened Gq-dependent proliferation of cardiac cells.

In this study, I attempted to determine whether cardiac–specific overexpression of Gαq would rescue the cardiac defects in ATE1-deficient mice. To this end, I constructed $ATE1^{-/-}$ $G\alpha q^{Tg}$ compound mutant mice, where Gαq is exclusively overexpressed in the heart from αMHC promoter. Morphological and histological analysis suggested that myocardial Gαq overexpression rescues significantly cardiac defects of $ATE1^{-/-}$ embryos in size and development of ventricular myocardium, ventricular septum, trabeculae, and atrium. While Gαq overexpression in the heart rescues significantly cardiac defects in ATE1-/- embryonic hearts, it did not cause a noticeable change in vascular defects, indicating, for the first time, cell-autonomous function of ATE1 in vascular development. These results together suggest that ATE1 controls cardiac development and signaling in part through regulated proteolysis of multiple regulators of Gq-activated signaling pathways.

2.2 BACKGROUND

The N-end rule pathway is one of ubiquitin (Ub)-mediated proteolytic system that relates the *in vivo* half-life of a protein to the identity of its N-terminal residue. Conjugation of arginine (Arg) by ATE1-encoded Arg-transferase to N-terminal aspirate (Asp), glutamate (Glu), or cysteine (Cys) is a posttranslational modification which creates the primary destabilizing residue Arg. The resulting N-terminal Arg of an arginylated substrate is subsequently recognized for protein ubiquitination by E3 Ub ligases, which produces a secondary degradation signal for processive degradation by the 26S proteasome complex. This universal eukaryotic protein modification, described 40 years ago (Kaji, Novelli et al. 1963), requires Arg from Arg-tRNA^{Arg} of the protein synthesis machinery and, thereby defines a tRNA-dependent Ub proteolytic system. In mammals ATE1 appears to be the only gene responsible for posttranslational arginylation as ATE1 knockout disrupts all known N-terminal arginylation processes (Kwon, Kashina et al. 2002). Characterization of ATE1-knockout mice demonstrated that they die at midgestation during embryogenesis primarily due to defects in cardiac development and angiogenesis. ATE1-deficient embryos at E12.5 started to show growth retardation associated with local hemorrhage in the midbrain or heart, swollen pericardial sac and edema under the dermal layer. Histological analysis of the hearts indicated thin ventricular myocardial hypoplasia and disorganized ventricular trabeculation, resembling thin myocardium syndrome (Jaber, Koch et al. 1996). The additional cardiac phenotypes of ATE1$^{-/-}$ embryos include a ventricular septal defect (VSD), a blood flow between the septum and endocardial cushion and also through fenestrations in the septal tissue itself. ATE1-/- embryos also exhibit a persistent truncus arteriosus, a common root of the aorta and pulmonary artery straddling a large VSD, with a

prevalence of 4 per 10,000 births in humans (Creazzo, Godt et al. 1998). In addition to cardiac defects, the majority of ATE1-/- embryos revealed vascular phenotypes including insufficiently branched and thinner vitelline vessels and prematurely terminated primary-plexus capillaries (Kwon, Kashina et al. 2002). These findings unveil unexpected physiological functions of the N-end rule pathway in cardiac development and angiogenesis in mammals.

Substrates of ATE1-dependent arginylation have remained unknown for the last four decades. In an attempt to identify the physiological substrates of ATE1 and other N-end rule components, a genome-wide functional proteomics was performed. In this assay, 18,000 cDNAs were individually expressed, labeled with biotin, and subjected to ubiquitination (Lee, Tasaki et al. 2005). Screening of ubiquitination substrates that are also sensitive to dipeptide inhibitors of the N-end rule pathway yielded ~35 candidate N-end rule substrates, including RGS4, RGS5 and RGS16 (Lee, Tasaki et al. 2005). Biochemical characterization in mouse embryonic fibroblasts (MEFs) indicated that these RGS proteins were ubiquitylated and degraded through ATE1-dependent arginylation, which required N-terminal second cystein (Cys-2) as a degron. RGS4 and RGS5 were rapidly ubiquitylated and degraded in MEFs, and their degradation was abolished in ATE1-/- MEFs (Lee, Tasaki et al. 2005). Mass spectrometric analysis of purified RGS4, overexpressed in MEFs, revealed Arg conjugation of N-terminal Cys-2, which has been exposed by Met aminopeptidases. Moreover, N-terminal Cys-2 itself was found to be conjugated with a mass of 48 Da (Kwon, Kashina et al. 2002). The interpretation for an additional mass was that 48-Da mass represents oxidation of Cys to Cys sulfonate ($CysO_3$), which was verified by the finding that depletion of oxygen *in vitro* and in mammalian cells disrupts degradation and ubiquitylation of RGS4 and RGS5 (Lee, Tasaki et al. 2005). Notably, the oxidized Cys residue (especially $CysO_2$) becomes structurally similar to Asp, a genuine substrate of ATE1 R-

transferase. N-terminally oxidized Cys should be recognized by UBR E3s for ubiquitylation and subsequent degradation by the 26S proteasome complex, yet the E3s involved remain incompletely understood. Recent studies demonstrated that UBR1-/-UBR2-/- mouse embryos die at midgestation associated with defects in cardiovascular development (An, Seo et al. 2006) and fail to degrade RGS4 and RGS5 (Lee, Tasaki et al. 2005). Although these results indicate that RGS4, RGS5 and RGS16 are biochemical substrates of the N-end rule pathway, it is unknown whether the O_2-dependent pathway controlling RGS proteolysis, and thus cardiac GPCR signaling, is present in cardiomyocytes.

Belonging to structurally related R4 subfamily of RGS proteins, RGS4, RGS5, and RGS16 are considered prototypical among RGS proteins, which negatively regulate GPCR signaling by converting the GPCR-activated, GTP-bound Gα subunit and Gβγ subunits into the GDP-bound, inactive Gαβγ heterotrimeric complex. Among the entire RGS proteins, RGS4 has received much attention as an important negative regulator of Gαq-mediated cardiovascular system, in part because RGS4 is prominently expressed in the myocardium (Kardestuncer, Wu et al. 1998; Adams, Pagel et al. 2000; Patten, Bunemann et al. 2002). RGS4 overexpression on the mRNA and/or protein level was frequently observed in the terminally failing myocardium from patients with dilated or ischemic cardiomyopathy with nonfailing controls or in some animal models with heart dysfunction (Zhang, Watson et al. 1998; Owen, Burton et al. 2001; Mittmann, Chung et al. 2002). RGS4 binding to Gαq inhibits Gαq-mediated PLCβ activation in the heart, suggesting that RGS4 is a PLCβ antagonist (Tamirisa, Blumer et al. 1999; Mittmann, Chung et al. 2002) (**Figure 3**). Stimulation of Gq-coupled receptors (e.g., by endothelin-1 receptor or α1-adrenoreceptor agonists), is involved in the development of cardiac hypertrophy and failure (D'Angelo, Sakata et al. 1997; Mende, Kagen et al. 1998). Recombinant RGS4 expression

inhibited endothelin-1-stimulated PLC activity in left ventricular myocardium (Mittmann, Chung et al. 2002). RGS4 overexpression in cardiomyocytes completely abolished the endothelin-1-induced increase in fractional shortening (Mittmann, Chung et al. 2002), and inhibited the effects of phenylephrine and endothelin-1 on ANF- and myosin light chain promoter activity and on phenylephrine-stimulated myofilament organization and cell growth (Tamirisa, Blumer et al. 1999).

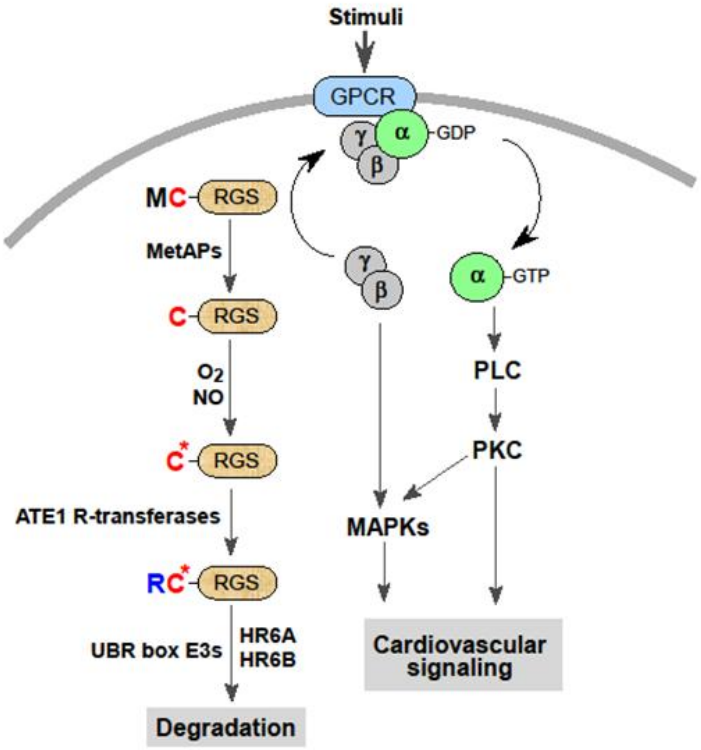

Figure 3. The proteolysis of RGS proteins and its role in cardiovascular signaling and homeostasis (Tasaki and Kwon 2007).

Transgenic mice overexpressing RGS4 in postnatal ventricular tissue displayed, upon transverse aortic constriction, reduced ventricular hypertrophy, left ventricular dilatation, depressed systolic function, and higher postoperative mortality, and failed to induce the normal fetal gene expression (Rogers, Tamirisa et al. 1999). Therefore, RGS4 overexpression in normal physiological condition would inhibit the beneficial hypertrophic response in the myocardium. However, in transgenic mice overexpressing both Gαq and RGS4, the development of contractile dysfunction, left ventricular dilatation, thinning of the left ventricular walls, and induction of the fetal gene expression was delayed (Rogers, Tsirka et al. 2001), suggesting that RGS4 overexpression alleviates pathologically hypertrophic response in the myocardium. Therefore, misregulation of RGS4 (RGS5 and RGS16 as well) level would disturb normal responses to physiological and pathological stimuli in the myocardium. Taken together, RGS4 (and probably RGS5 and RGS16 as well) appears to regulate the basal and agonist-stimulated Gαq signaling in the myocardium and to regulate myocardial hypertrophy and contractility. However, the cellular mechanisms of regulation of the RGS proteins level are currently elusive. In addition to the potential function of RGS5 in the myocardial growth, RGS5 is prominently expressed in vascular smooth muscle cells and pericytes (Adams, Pagel et al. 2000; Kirsch, Wellner et al. 2001; Bondjers, Kalen et al. 2003; Cho, Kozasa et al. 2003; Furuya, Nishiyama et al. 2004) and has been implicated in capillary growth and angiogenesis (Wieland and Mittmann 2003; Hamzah, Jugold et al. 2008). RGS5 was also suggested to act as a GAP (GTPase activating protein) for Gαi and Gαq and attenuates Ca^{2+} and ERK signals induced by angiotensin II, endothelin-1, sphingosin-1-phosphate, and PDGF in cultured cells (Zhou, Moroi et al. 2001; Cho, Kozasa et al. 2003). Taken together, RGS5 seems to be an important counter regulator for the Gαq-mediated

signaling in the vascular system as well. Although several studies have implicated RGS16 in the endotoxin-induced heart failure and PLC inactivation (Patten, Bunemann et al. 2002), it appears to play a role in lymphocyte migration as well (Lippert, Yowe et al. 2003).

The BrdU incorporation assay performed on developing hearts and cardiac cells of +/+ and $ATE1^{-/-}$ embryos showed that ATE1 null cardiac defects are directly linked to cardiac proliferation and signaling rather than a secondary effect to non-cardiac defects (Lee, Kwon et al. unpublished). The levels of cells in the S-phase were significantly decreased in ventricular wall and intraventricular septum, but not in trabeculae of ATE1 null embryos. The BrdU index was profoundly reduced in troponin I (a marker for cardiomyocyte)-positive $ATE1^{-/-}$ cardiomyocytes (~9.4%) compared to those (~20%) of $ATE1^{+/+}$ cardiomyocytes. Cardiomyocyte-specific expression of NLS-lacZ (β-galactosidase N-terminally fused with a nuclear localization signal), marked into the ATG codon of ATE1 gene, suggested that ATE1 has a cell-autonomous function in cardiac proliferation. Whole-mount staining detected significantly stabilized endogeneous RGS4 in $ATE1^{-/-}$ embryos and sectional immunohistochemistry exhibited robust RGS4 signal in $ATE1^{-/-}$ embryonic hearts (Lee, Kwon et al. unpublished), indicating RGS4 functions are tightly controlled by posttranslational arginylation. In an attempt to identify Gq agonists whose functions are linked to ATE1, the proliferation of +/+ and ATE1-/- cardiac cells was monitored after the treatment of various GPCR agonists, including PGF2α (prostraglandin F receptor coupled with Gq), phenylephrine (α-adrenergic receptor coupled with Gq and Gi), FGFb (FGF basic receptor which is a receptor tyrosine kinase), ISO (β-adrenergic receptor coupled with Gs), and angiotensin II (AngII, AT1 receptor coupled with Gq and Gi). Amonst these GPCR agonists, AngII treatment increased significantly cardiac proliferation in +/+ cardiomyocytes, whereas AngII-induced proliferation was prominently reduced in ATE1-/- cardiomyocytes (Lee, Kwon et

al. unpublished).

Based on these results, I employed genetic dissection to determine the role of ATE1 in Gq-dependent cardiac signaling. To this end, I crossed ATE1+/- mice and Gαq transgenic mice (D'Angelo, Sakata et al. 1997) and asked whether overexpression of Gαq in the heart would significantly rescue cardiac null phenotypes in ATE1-/- embryos. Consistent with previous observations (Kwon, Kashina et al. 2002), gross morphology of $ATE1^{-/-}$ embryos at E14.5 through E16.5 exhibited growth retardation, local hemorrhages and swollen pericardial sac. Gross morphology of hearts of $ATE1^{-/-}$ and $ATE1^{-/-}G\alpha q^{Tg}$ was largely comparable at E14.5 and E15.5. However at E16.5, the development of hearts between ATE1-/- and ATE1-/-$G\alpha q^{Tg}$ showed obvious difference. Whereas $ATE1^{-/-}$ hearts at E16.5 are morphologically defective, ATE1-/-$G\alpha q^{Tg}$ hearts at same stage resembled, at least significantly and to a varying degree, those of littermate wild-type and Gαq embryos. Cross section of embryonic hearts suggested that ATE1 null cardiac defects in size, myocardium, ventricular septum, trabeculae and atrium were significantly rescued by Gαq overexpression. These results together indicate that posttranslational arginylation plays an important role in cardiac Gq-signaling pathways.

2.3 METHODS

Construction of $ATE1^{-/-}G\alpha q^{Tg}$ mice. All animal studies were in accordance with protocols approved by the Institutional Animal Care and Use Committee at University of Pittsburgh. We obtained Gαq transgenic mice expressing 40 copies of Gαq transgene from α-

myosin heavy chain (MHC) on FVB/N background in collaboration with Dr. Gerald Dorn II at the University of Cincinnati (D'Angelo, Sakata et al. 1997). I constructed $ATE1^{-/-}G\alpha q^{Tg}$ mice by crossing $ATE1^{+/-}$ mice (Kwon, Kashina et al. 2002) with Gαq transgenic mice. Mice lacking ATE1 was as previously described (Kwon, Kashina et al. 2002). Embryos at E14.5 to E16.5 were obtained from timed mating of ATE1+/- mice with Gαq transgenic mice. The presence of a vaginal plug after overnight mating was regarded as E0.5.

Genotyping. Genotyping of the yolk sac or tail genomic DNA from each embryos or mice was performed by standard PCR using the following condition: one cycle at 94°C 2min, 20 cycles of 94°C 20s, 56°C 20s, 65°C 30s, 10 cycles of 94°C 20s, 56°C 20s, 65°C 1min, 10 cycles of 94°C 20s, 56°C 20s, 65°C 1min 30s and a final extension step at 65°C for 2min. The primers used for detecting ATE1 were AK49 5'-GGTATTTGCTGCCGTCCTTTGGTGGT-3' (forward), AK83 5'-CTGGAGACAAAGCCCCAGCCAGAC-3' (reverse), and YT655 5'-CCAGCTCATTCCTCCCACTCATGATC-3' (reverse), respectively amplifying 570-bp and 430-bp fragments for the wild type allele and knockout allele, respectively. The primers used for detecting Gαq are MHC5A 5'-CAGGACTTCACATAGAAGCC-3' (forward) and G4 5'-CGTGAAGATGTTCTGATACAC-3' (reverse), amplifying 500-bp of transgene.

Histology. Embryonic hearts were dissected in cold PBS and fixed overnight at 4°C in 4% paraformaldehyde (Fisher Scientific) in PBS. Samples were stored in 70% ethanol at 4°C after several washing with PBS. For histological analysis, samples were dehydrated in serial ethanol, cleared in histosol (National Diagnostics), paraffin-embedded, sectioned transversely at 5μm, and stained with hematoxylin and eosin (H&E).

Western Blot. Embryonic hearts or other tissues (brain, liver, lung) at E15.5 were dissected in cold PBS and homogenized in RIPA lysis buffer (150mM Sodium Chloride, 1% NP-40, 0.5% Sodium deoxycholate, 0.1% SDS, 50mM Tris, pH 8.0) including protease inhibitor cocktail (Sigma). Protein concentrations were determined using the BCA protein assay (Pierce, Rockford, Ill.) with bovine serum albumin as a standard. 20ug of total protein extracts from each tissue were subjected to electrophoresis and transfered to polybvinylidene fluoride (PVDF) membrane, and stained with anti-Gαq antibody (Santa Cruz), followed by re-staining with anti-β-actin antibody (Sigma) as a loading control. Gαq expression was quantitated by densitometry (Image J software) followed by normalization with β-actin signal.

2.4 RESULTS

To genetically determine whether myocardial-specific Gαq overexpression would rescue ATE1 null cardiac defects, I constructed $ATE1^{-/-}Gαq^{Tg}$ mice by crossing ATE1+/- mice in the C57BL/6J-129SvEv backgrounds with Gαq transgenic mice in the FVB/N background, where Gαq is overexpressed from the α-myosin heavy chain (MHC) promoter.

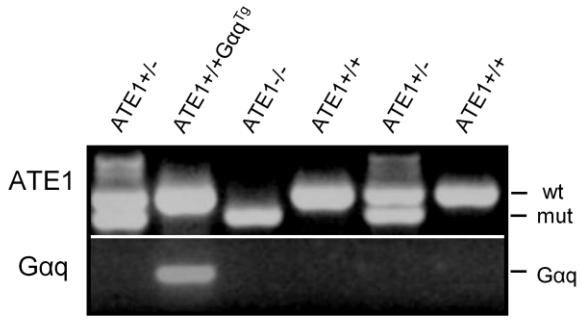

Figure 4. The genotyping of embryos from intercross between ATE1+/- and Gq^{Tg} mice. Yolk sac genomic DNA was isolated from embryos and PCR was performed using two sets of primer. DNA bands corresponding to the ATE1 alleles for wild-type (wt) and mutant (mut) and αMHC-Gαq transgene (Gαq) are indicated on the right.

I observed approximately 100 embryos at E14.5 through E16.5 from the timed-mating and determined the gross morphology and the timing of cardiac defects. Genotyping was performed by standard PCR using the yolk sac genomic DNA of embryos (**Figure 4**). Two separate sets of primers to detect the wild-type and knock-out *ATE1* alleles and the αMHC-Gαq transgene are respectively AK49/AK83/YT655 and MHC5A/G4. Immunoblotting of compound mutant embryos at E15.5 showed that Gαq was overexpressed only in the heart by ~5-fold, but not in other tissues such as liver, lung and brain (**Figure 5**). It has been recently observed that $ATE1^{-/-}$ embryos at the stages up to E11.5 were recovered approximately at Mendelian ratios but developmentally retarded from E12.5 (Lee, Kwon et al. unpublished). No embryos were retrieved alive beyond E15.5. However, in the mixed background of C57BL6/129S and FVB/N, I found that the onset of overall phenotype was delayed by 2~3 days and the resulting phenotypes are somewhat moderate. At E15.5 and E16.5, some of ATE1-deficient embryos (60% and 43% respectively) were still alive (**Table 1**).

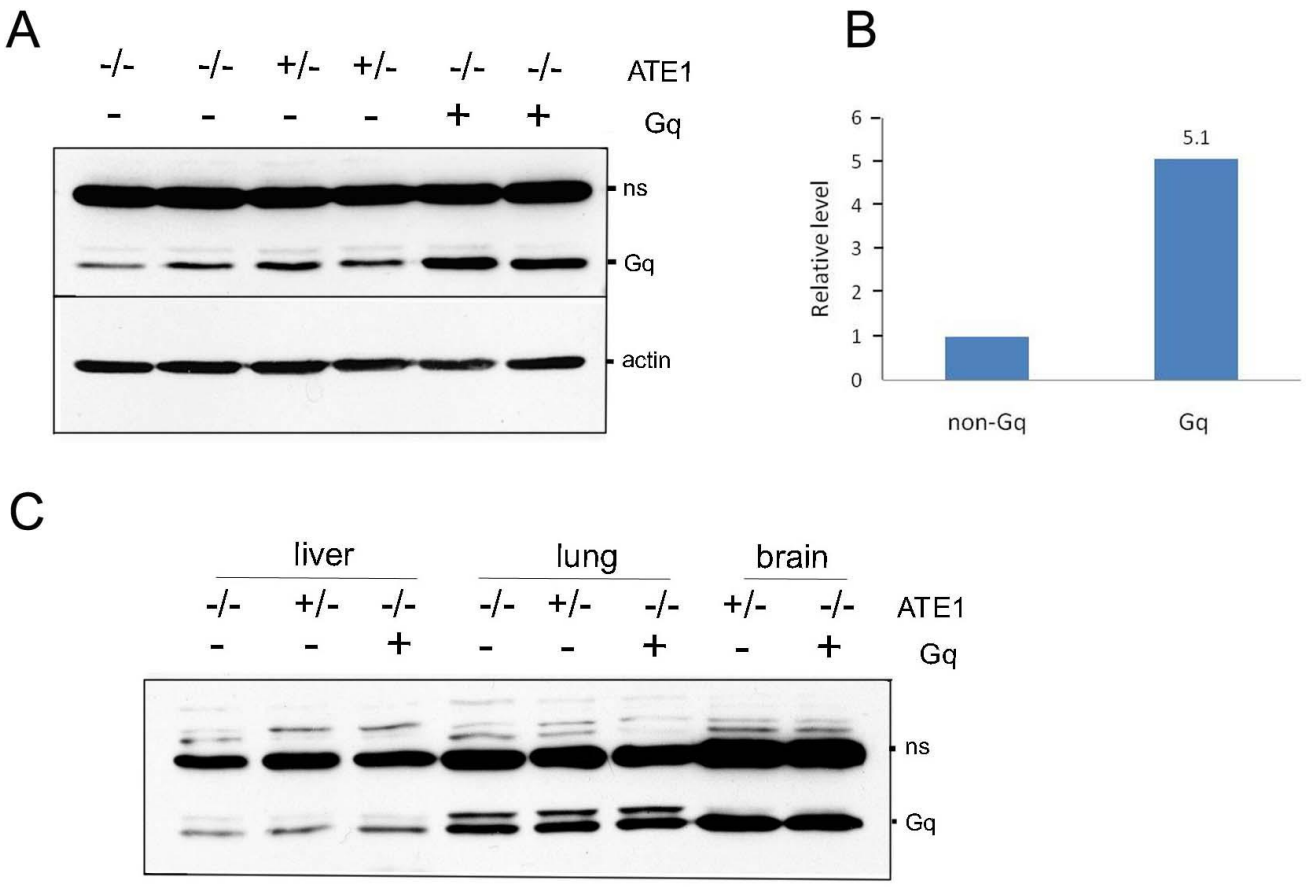

Figure 5. Immunoblotting of Gαq from intercross between ATE1+/- and Gαq^{Tg} mice. (A) Gαq protein expression in embryonic hearts at E14.5. Anti-β-actin antibody was used to confirm an equal loading. (B) Quantitative Gαq protein expression normalized to β-actin (shown as fold induction over NTG animals) (n=2 in each group) (C) Gαq protein expression in liver, lung and brain of embryos at E14.5. Labeled bands correspond to the followings: ns, nonspecific; Gq, Gαq^{Tg}.

Table 1. Genotype analysis of embryos from crossing between ATE1+/- and Gαq^{Tg} mice

	E14.5	E15.5	E16.5
ATE1+/+	3	7	3
ATE1+/-	8	5	14
ATE1-/-	5 (2 inviable)	5 (2 inviable)	7 (4 inviable)
Gαq^{Tg}	2	1	4
ATE1+/-Gαq^{Tg}	4	5	9
ATE1-/-Gαq^{Tg}	4 (2 inviable)	3 (2 inviable)	8 (5 inviable)

However, as previously reported (Kwon, Kashina et al. 2002) Lee, Kwon et al. unpublished), the majority (~76%) of ATE1$^{-/-}$ embryos at E14.5 through 16.5 exhibited the growth retardation associated with a local hemorrhage in the brain, blood leakage into the pericardial cavity, and edema under the dermal layer, in comparison with littermate controls (**Figure 6**). Comparable number (~73%) of ATE1$^{-/-}$Gαq^{Tg} embryos also showed same phenotype (**Figure 6**).

Gross vascular phenotype of ATE1$^{-/-}$ embryonic yolk sacs exhibited poorly developed and sparse vitelline vessels and pale yolk sacs, as did ATE1$^{-/-}$Gαq^{Tg} (**Figure 7**). These results indicated that vascular defects in both yolk sacs and embryos were not affected significantly by myocardial Gαq overexpression.

Gross heart morphology of ATE1-/- and ATE1$^{-/-}$Gαq^{Tg} embryos at E14.5 and E15.5 were largely comparable to wild-type or Gαq^{Tg} with some individual variations, although they had smaller hearts (**Figure 8**). However, by E16.5, the development of ATE1$^{-/-}$Gαq^{Tg} hearts (n=8)

became apparently equivalent to littermate wild-type and $G\alpha q^{Tg}$ embryos, whereas ATE1-/- hearts at the same stage were morphologically defective and exhibited cone-like shape (**Figure 8**).

To confirm the above-mentioned observations, we examined internal morphology of embryonic hearts at E14.5 through E16.5 by H&E staining. Transverse sections of embryonic hearts demonstrated that both $ATE1^{-/-}$ and $ATE1^{-/-}G\alpha q^{Tg}$ at E14.5 have impaired cardiac phenotype showing ventricular septal defect (VSD), ventricular hypoplasia and poor trabecular formation (**Figure 9A~D**). By E15.5, however, interventricular septum in $ATE1^{-/-}G\alpha q^{Tg}$ hearts grew toward the atrioventricular cushion tissue (**Figure 9E~G)** and subsequently fused with the myocardial tissue resulting in completely closed septum by E16.5 (**Figure 10**). In addition to VSD, the cardiac defects including thin myocardium and poor trabeculae were rescued in 4 out of 5 hearts when observed between E15.5 and E16.5. The thickness of compact zone of the left ventricle in E16.5 $ATE1^{-/-}G\alpha q^{Tg}$ hearts was 13~17-cells, which is comparable to $ATE1^{+/+}$ (10~12-cells) and $G\alpha q^{Tg}$ (10~14-cells), whereas $ATE1^{-/-}$ hearts displayed 1~6-cells-thickness at same developmental stage (**Figure 11**). The atria (data not shown) and major cardiac vessels such as aorta and pulmonary artery between genotypes did not display any significant difference (**Figure 12**).

Based on these results, I conclude that cardiac-specific Gαq overexpression rescues significantly cardiac defects in $ATE1^{-/-}$ embryos. In contrast to cardiac defects, Gαq overexpression in the heart did not affect invariably vascular defects of $ATE1^{-/-}$ at E14.5 through E16.5, suggesting that ATE1 plays a cell-autonomous function in vascular signaling.

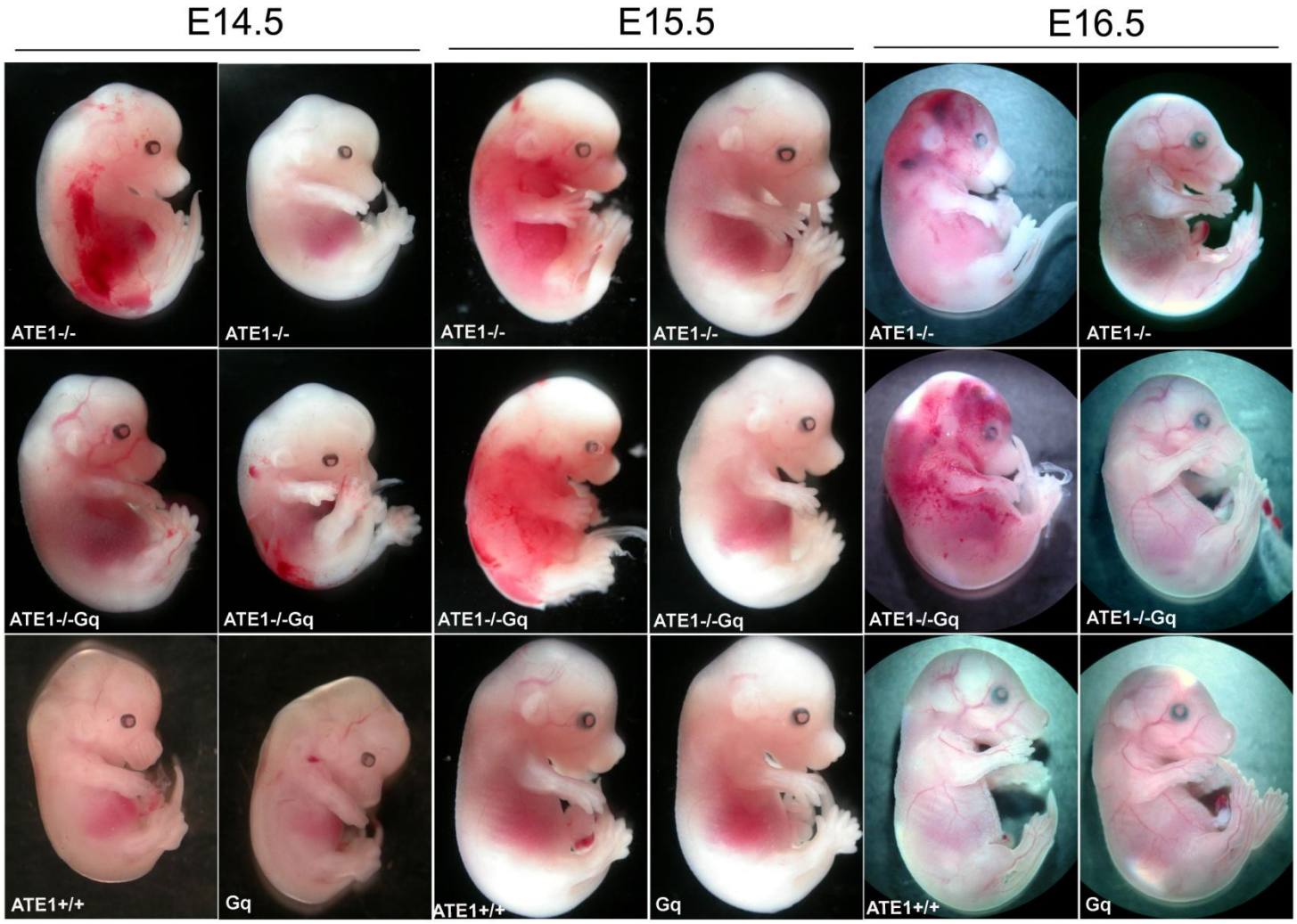

Figure 6. Gross morphology of embryos at E14.5 through E16.5.

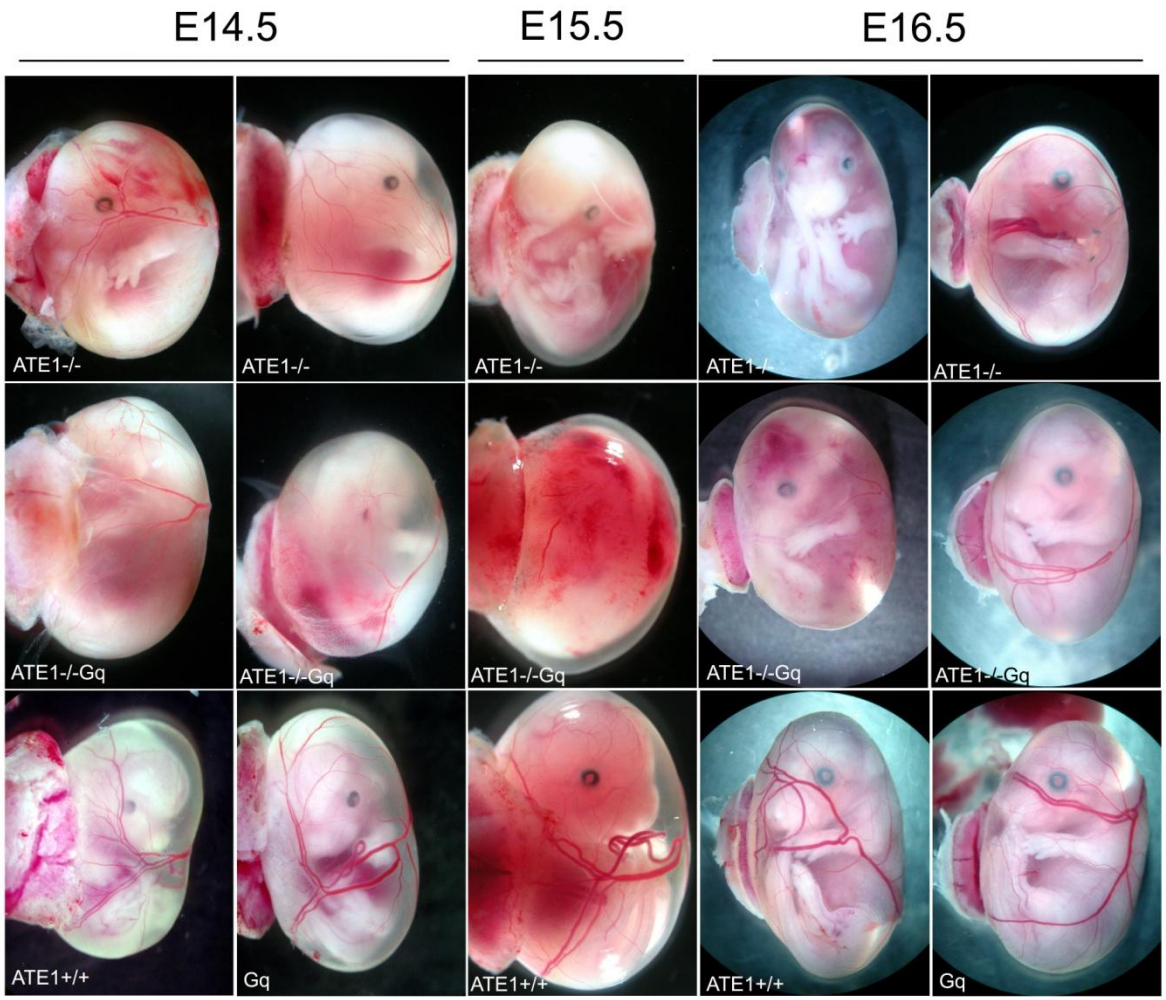

Figure 7. Gross morphology of yolk sacs at E14.5 through E16.5, in which vascular defects are obvious in ATE1$^{-/-}$ and ATE1$^{-/-}$Gq^{Tg}.

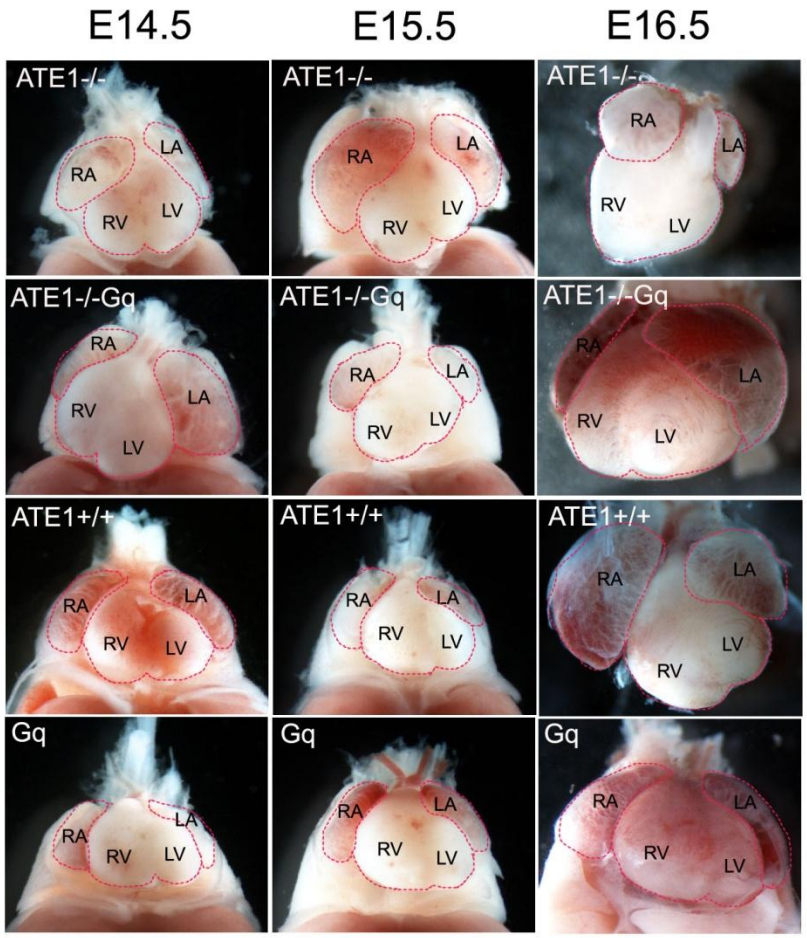

Figure 8. Gross morphology of embryonic hearts at E14.5 through E16.5. RV, right ventricle; LV, left ventricle; RA, right atrium; LA, left atrium.

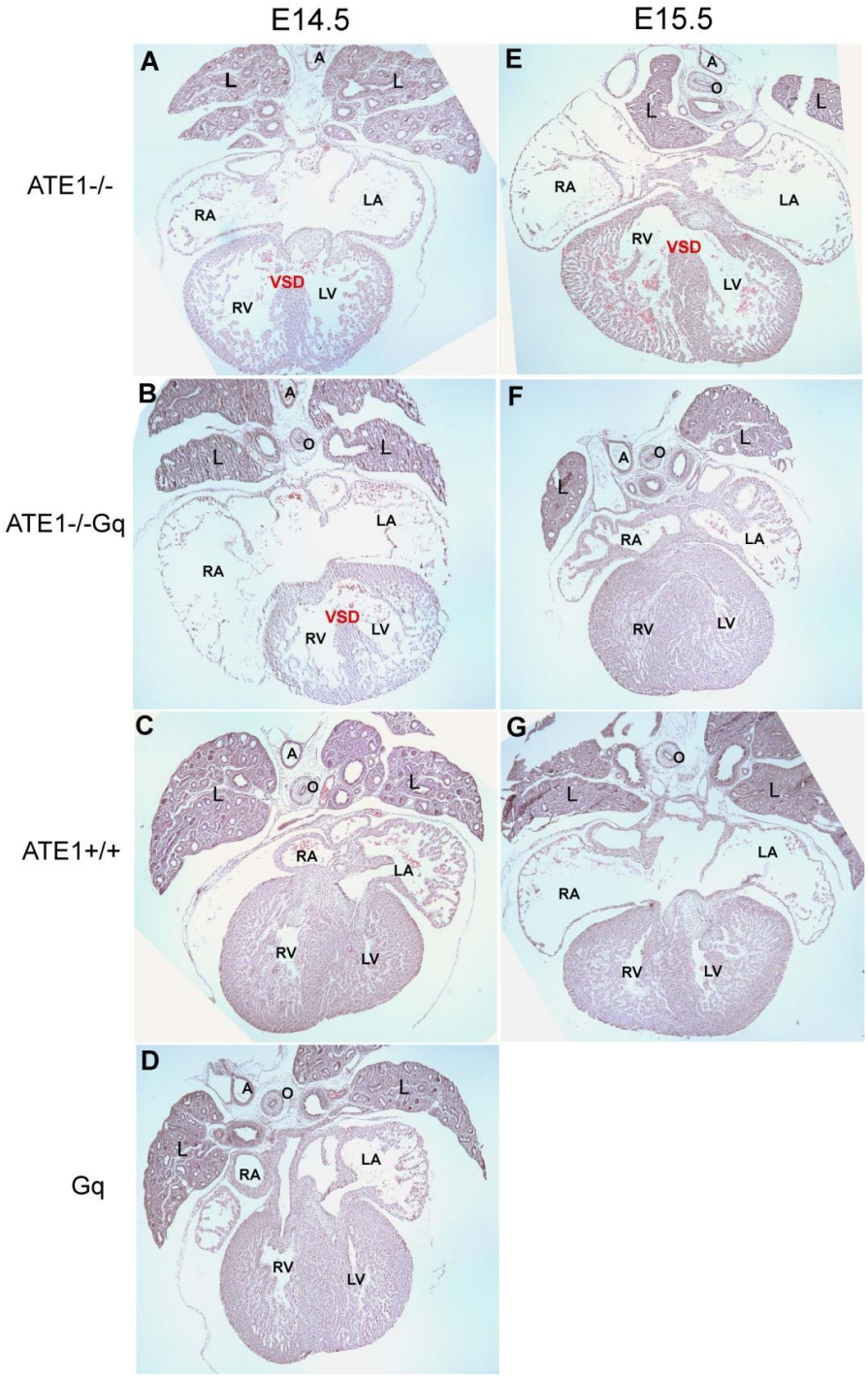

Figure 9. Internal morphology of embryonic hearts at E14.5 and E15.5. H&E-stained transverse sections of embryonic hearts at different stages. L, liver; A, aorta; O, oesophagus; RA, right atrium; LA, left atrium; RV, right ventricle; LV, left ventricle; VSD, ventricular septal defect. Magnification x40

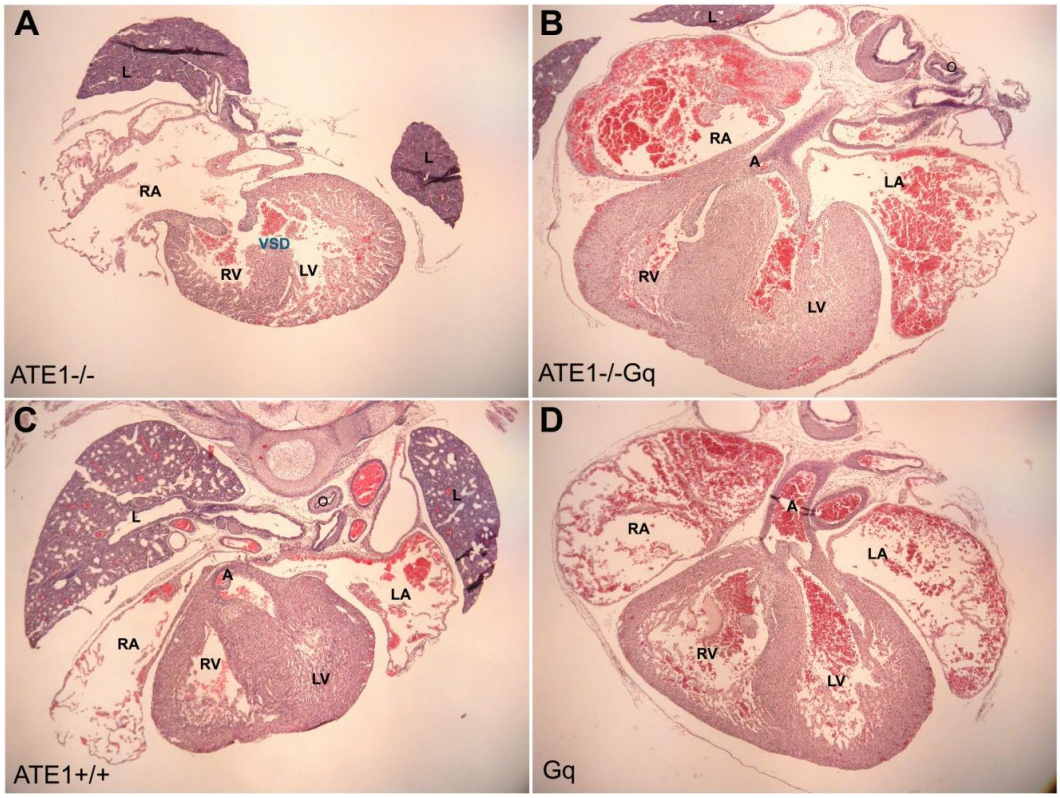

Figure 10. **Internal morphology of embryonic hearts at E16.5.** H&E-stained transverse sections of embryonic hearts. L, liver; A, aorta; O, oesophagus; RA, right atrium; LA, left atrium; RV, right ventricle; LV, left ventricle. Magnification x40.

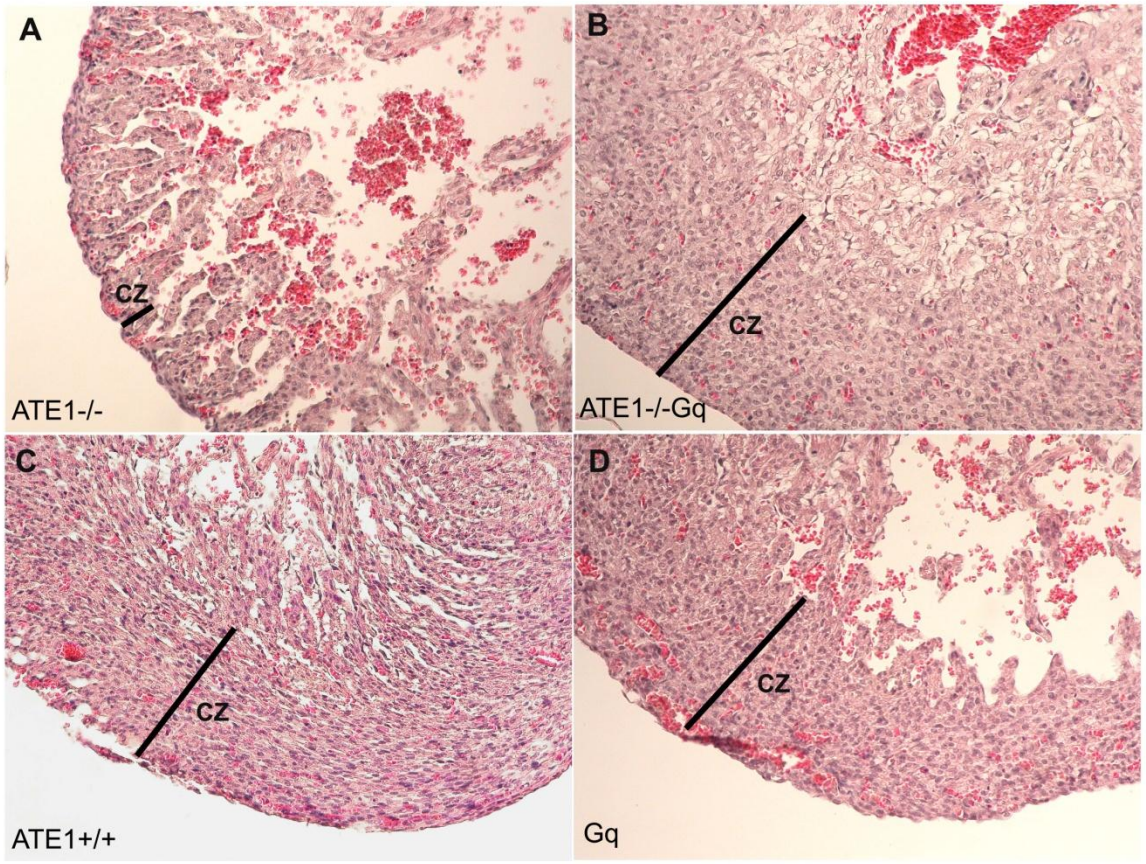

Figure 11. Histological analysis of left ventricular myocardium. The thickness of compact zone in left ventricle myocardium was compared between different genotypes. CZ, compact zone. Magnification x200

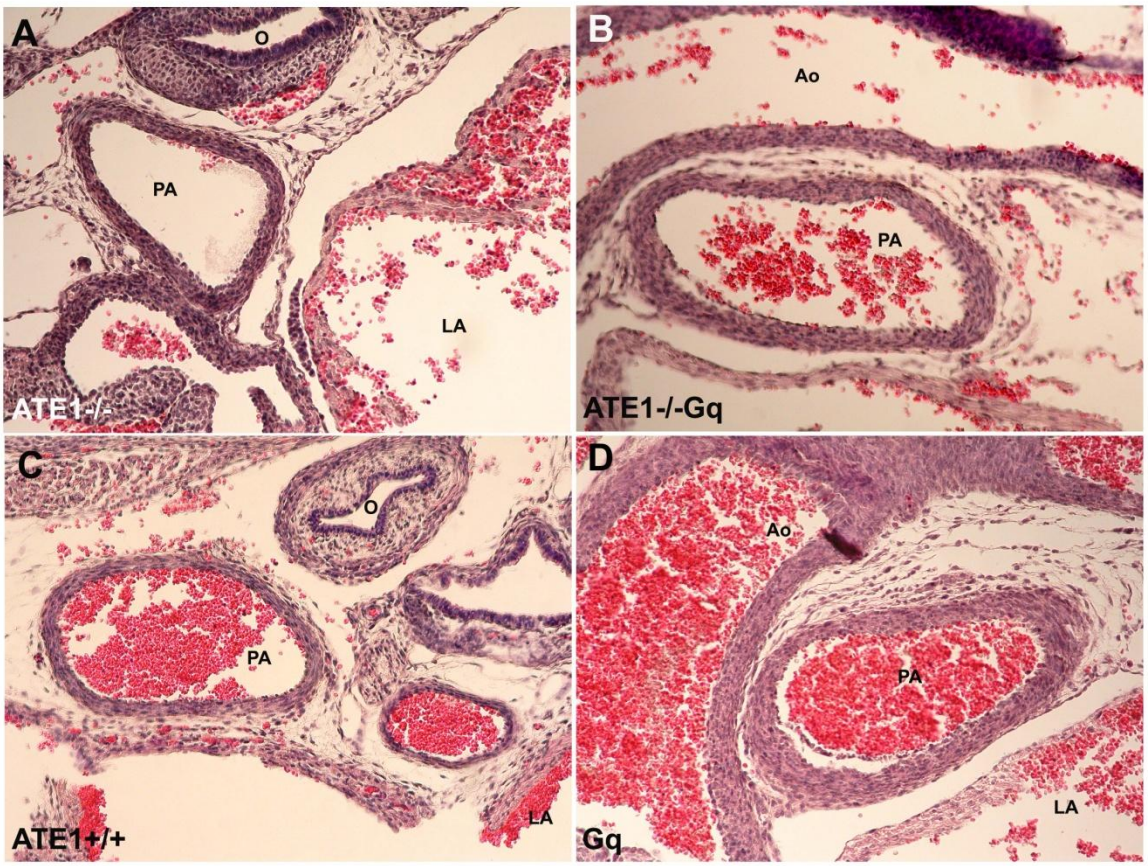

Figure 12. Arterial phenotype of embryos at E16.5. H&E-stained transverse sections of embryonic hearts. Ao, aorta; PA, pulmonary artery; LA, left atrium; O, oesophagus. Magnification x200

2.5 DISCUSSION

ATE1 mediates arginylation, a universal eukaryotic protein modification, in N-terminal Cys as well as Asp and Glu of proteins. ATE1-deficient mice die during embryogenesis associated with ventricular myocardial hypoplasia, disorganized ventricular trabeculation, thin myocardium syndrome, and angiogenetic defects (Kwon, Kashina et al. 2002). Recent data suggested that significantly reduced proliferation of cardiomyocytes in ATE1$^{-/-}$ hearts mainly attributes to the cardiac defects in a manner depending on cardiac Gq signaling (Lee, Kwon et al. unpublished). In this study, I determined the role of ATE1 at the molecular level in cardiac Gq signaling and development. I found that transgenic overexpression of Gαq partially rescued cardiac defects but not vascular defects of ATE1-deficient mice, as determined by overall size, morphology and histological analysis of H&E stained cardiac sections. Although cardiac Gαq overexpression didn't influence the gross morphology of ATE1-/- embryos including growth retardation or local hemorrhages, embryonic heart sections revealed that ATE1 null cardiac defects such as VSD and thin myocardium were significantly rescued by Gαq overexpression. Recent work has discovered new physiological functions of N-terminal arginylation in adult mice (Brower and Varshavsky 2009). The postnatal deletion of mouse Ate1 using Cre/lox technique induced growth retardation resulting in early death of ATE1-deficient mice. They displayed a strikingly lower white adipose tissue (WAT) and they are resistant to high-fat diet-induced obesity due to the ectopic induction of Ucp1 in WAT. In addition, they have a kyphotic posture (a forward rounding of the upper back) and disproportionately large brains contributed by cerebral edema, in comparison to those of control siblings. They exhibited the neurological/behavioral abnormality including hyperactivity and higher liability to seizure.

Moreover, postnatally ATE1-deficient mice show male-specific infertility with few sperm cells in disorganized arrangement. Taken all together, arginylation by ATE1 involves in broad range of physiological process including spermatogenesis, adipogenesis, and neurogenesis, as well as cardiovascular development.

The genetic background of mutant animals influences the phenotypes observed to a greater or lesser extent (Jackson and Abbott 2000). The issue of genetic background has particularly been raised in neurosciences, regarding the complex behavioral phenotypes. Some literatures have shown that genetic background markedly influences the severity of phenotypes in broad range of biomedical fields including cardiovascular research (Schlager 1966; Blizard and Welty 1971; Hoit, Kiatchoosakun et al. 2002; Tominaga, Matsuda et al. 2004; Heydemann, Huber et al. 2005). One example is two distinct transgenic lines expressing hypertrophic cardiomyopathy-linked mutant tropomyosin E108G showing drastically different phenotypes. One created on the FVB/N background displayed relatively mild diastolic dysfunction (Michele, Gomez et al. 2002) and the other on the C57BL/6J background developed obvious hypertrophic cardiomyopathy and heart failure (Prabhakar, Boivin et al. 2001). As described in these finding, C57BL/6J is more susceptible to revealing cardiac phenotype than FVB/N, which may explain why the onset of phenotype in ATE1-/- embryos on mixed background between C57BL6/129S and FVB/N was overall delayed and rather milder than on C57BL6/129S.

I observed that the internal cardiac morphology of $ATE1^{-/-}G\alpha q^{Tg}$ mice exhibited dilated ventricles compared to wild-type controls (**Figure 10**). It has been known that transgenic mice overexpressing wild-type Gαq in the heart using the α-myosin heavy chain promoter demonstrated cardiac hypertrophy, depending on the level of overexpression, with marked increases in markers of hypertrophy and heart failure and revealed impaired intrinsic contractility

(D'Angelo, Sakata et al. 1997). High levels (40-copies, approximately five-fold excess Gαq protein over endogenous levels) of Gαq overexpression can lead to a dilated cardiomyopathy, which is the consequence of lethal congestive heart failure (D'Angelo, Sakata et al. 1997). As previously reported, in this study, $ATE1^{-/-}Gαq^{Tg}$ and $Gαq^{Tg}$ mice overexpressing 40 copies of transgenes showed mortality on the mixed background (FVB/N X C57J/129S) as well. I observed that $ATE1^{-/-}Gαq^{Tg}$ hearts together with $Gαq^{Tg}$ developed enlarged ventricles and showed the hint of cardiomyocyte hypertrophy on left ventricles. The hypertrophy of $ATE1^{-/-}$ $Gαq^{Tg}$ hearts indicates that high copy number of Gαq in compound mice induced hypertrophy exceeding the rescue of cardiac defect of $ATE1^{-/-}$ embryos.

3.0 THE N-END RULE PATHWAY IN RGS5 UBIQUITINATION AND CARDIOVASCULAR SIGNALING

3.1 OVERVIEW

RGS5, which has been identified as N-end rule substrate through genomewide functional proteomic screening, is known to play a role in negatively regulating G protein-coupled receptor (GPCR) signaling in the hearts and blood vessels. As one of R4 family, RGS5 exhibits prominent expression in vascular smooth muscle cells and pericyte and has been recently identified as a key regulator for blood pressure regulation, vascular remodeling, and pericyte maturation in tumors. The biochemical analyses in mouse embryonic fibroblasts (MEF) have previously shown that ubiquitination of RGS5 involves Cys-2 as a degradation determinant and is impaired by hypoxic treatment, indicating that RGS5 proteolysis may act as an O_2 sensor controlling cardiovascular homeostasis. In this study, I generated RGS5 transgenic mouse strains overexpressing either MC-RGS5 (wild-type, short-lived) or MV-RGS5 (mutant, long-lived) from vascular smooth muscle-specific SM22α promoter to determine the physiological importance of RGS5 proteolysis in Gq signaling of VSMC. The results from transient transfection using

transgenic constructs showed that MC-RGS5 (wild-type) expressed from the SM22α promoter is rapidly degraded in rat aortic smooth muscle cells (A7r5), while the mutation of RGS5 Cys-2 to Val results in an increased steady state level of RGS5. Both MC-RGS5 and MV-RGS5 mice were viable and fertile without any visible defects. Gross morphology of embryos from both transgenic mice did not exhibit any significant phenotype compared to non-transgenic siblings. However, MC-RGS5 female transgenic mice demonstrated impaired delivery in that newborn pups were often found dead associated with a reduced level or the total absence of milk in their stomachs, whereas MV-RGS5 mice never showed this phenotype. This phenotype mimics that of oxytocin null mice, indicating that RGS5 may negatively regulate oxytocin receptor which is one of Gq-protein coupled receptor. The mis-regulation of this RGS5 function may result in the failure in oxytocin-induced uterine and mammary gland smooth muscle contraction. This transgenic model will be useful in testing a model where the steady state level of RGS5 in vascular smooth muscle cells (VSMC) of blood vessels as well as uterine SMC is regulated by the N-end rule pathway through its posttranslational modifications such as oxidation, arginylation, ubiquitination and degradation and provide a molecular basis in homeostasis of cardiovascular Gq signaling.

3.2 BACKGROUND

RGS5 (Regulators of G-protein Signaling 5) was identified, together with RGS4 and RGS16, as a substrate of N-end rule pathway through genome-wide functional proteomics.

RGS5 has been known to negatively regulate GPCR signaling as a GTPase activating protein (GAP) for Gαi and Gαq by converting the GPCR-activated, GTP-bound Gα subunit and the Gβγ subunits into the GDP-bound, inactive Gαβγ heterotrimeric complex. RGS5 attenuates angiotensin II and endothelin-1-induced intracellular Ca^{2+} transients in 293T cells. The translocation of RGS5 from cytosol to plasma membrane requires its N terminal extension (aa 1-33), which is not essential for exerting inhibitory activities (Zhou, Moroi et al. 2001). In addition, RGS5 suppresses ERK signals induced by angiotensin II, endothelin-1, sphigosin-1-phosphate, and PDGFββ in NIH-3T3 cells, suggesting that RGS5 inhibits signaling through GPCR as well as through PDGFR (Cho, Kozasa et al. 2003). Microarray analysis to identify markers in artery revealed RGS5 as one of the most prominent markers in pericytes of capillary vessels and VSMC of larger vessels (Adams, Pagel et al. 2000; Kirsch, Wellner et al. 2001; Bondjers, Kalen et al. 2003; Cho, Kozasa et al. 2003; Furuya, Nishiyama et al. 2004). RGS5 is prominently expressed in cells associated with the abluminal side of the endothelium rather than the endothelial cells. In the brain and arterial blood vessels of embryos, RGS5 colocalizes with pericyte markers, PDGFRβ and NG2 chondroitin sulfate proteoglycan. VSMC around arteries and arterioles and kidney mesangial cells show prominent RGS5 expression, whereas veins show limited or undetectable levels of RGS5 expression (Bondjers, Kalen et al. 2003). In adult mice, RGS5 expression is induced in VSMC of arteries during neovascularization associated with skin wound-healing, ovulation and tumor angiogenesis (Furuya, Nishiyama et al. 2004; Berger, Bergers et al. 2005), indicating the role of RGS5 in active vessel remodeling.

As shown in structurally-related RGS4 proteolysis, RGS5, one of substrates of ATE1-dependent arginylation, was rapidly degraded when expressed in reticulocyte lysates and metabolically stabilized by the proteasome inhibitor MG132 or the type-1 dipeptide N-end rule

inhibitor Arg-Ala (Lee, Tasaki et al. 2005). RGS5 was short-lived in mouse embryonic fibroblasts (MEF) as determined by pulse chase analysis, and its degradation was disrupted by the treatment of MG132. RGS5 was also metabolically stabilized in $ATE1^{-/-}$ MEF or by mutations of Cys-2 to stabilizing residues, Val or Ala, suggesting that *in vivo* RGS5 degradation depends on ATE1-dependent arginylation. Biochemical analyses demonstrate that arginylated RGS5 is subsequently recognized by N-recognins, including UBR1 and UBR2, for ubiquitination and degradation by the 26S proteasome complex. Consistent with these results, mouse embryos lacking UBR1 and UBR2, two functionally overlapping E3s, die at midgestation associated with defects in cardiovascular development (An, Seo et al. 2006), and MEFs derived from these embryos are impaired in the ability to degrade RGS4 (Lee, Tasaki et al. 2005). The degradation and ubiquitination of normally short-lived RGS5 was significantly decreased upon hypoxic condition, in contrast to the level of the long-lived C2A-RGS5 mutant, which was not affected by O_2 depletion (Lee, Tasaki et al. 2005). Mass spectrometry analysis found that the molecular mass of the Cys-2 residue of arginylated RGS4 purified from mouse L cells was increased by 48 Da (Kwon, Kashina et al. 2002), suggesting that the N-terminal Cys-2 residue of RGS4 (exposed at the N-terminus by Met aminopeptidases) may be oxidized into $CysO_2$ or $CysO_3$. Given that oxygen is essential for the proteolysis of RGS5 which is structurally related to RGS4, RGS5 may undergo the same posttranslational modification including arginylation and oxidation. These results suggest that ATE1-dependent pathway may be an O_2 sensor that controls cardiovascular homeostasis through oxidation, arginylation, ubiquitination, and subsequent degradation of RGS5.

Recently RGS5-deficient mouse strains were created by two laboratories (Cho, Park et al. 2008; Nisancioglu, Mahoney et al. 2008). RGS5-deficient mice exhibit hypotension associated

with slightly dilated aortas without detectible defects in vascular development (Cho, Park et al. 2008; Nisancioglu, Mahoney et al. 2008). To assess whether RGS5 is required for normal BP homeostasis, the tail BP of awake $^{+/+}$ and *RGS5*$^{-/-}$ mice was monitored. Studies with *RGS5*$^{-/-}$ mice showed that female mutants have lower BP than male mutants. Specifically, the mean arterial pressure (MAP) of five male *RGS5*$^{-/-}$ mice was 116 ± 6 mmHg which was significantly lower than 145 ± 5 mmHg of wild-type littermate controls (P-value=0.005). The average MAP of three female *RGS5*$^{-/-}$ mice was 84 ± 1 mmHg compared with 144 ± 9 mmHg for wild-type littermate controls (P-value=0.003). The examination of the ascending, mid-thoracic aorta and proximal to the diaphragm suggested that the low BP of RGS5-deficient mice can be attributed at least in part to dilated aorta. Another group genetically induced pancreatic carcinoma in RGS5-deficient mice, exhibiting reduction in tumor hypoxia and vessel leakiness associated with pericyte maturation and vascular normalization (Hamzah, Jugold et al. 2008). These *in vivo* animal models indicate that RGS5 plays a pivotal role in blood pressure regulation and vascular remodeling.

In this study, to determine the physiological role of RGS5 proteolysis in vascular signaling, I constructed RGS5 transgenic mouse strains, overexpressing either wild type RGS5 (MC-RGS5) or mutant RGS5 (MV-RGS5) from the vascular smooth muscle-specific SM22α promoter. The results from transient transfection using the transgenic constructs showed that MC-RGS5 (wild-type) expressed from the SM22α promoter is rapidly degraded in rat aortic smooth muscle cells (A7r5), while the mutation of RGS5 Cys-2 to Val results in an increased steady state level of RGS5. This suggests that Cys-2-dependent degradation of RGS5 is regulated by N-end rule pathway. Genotyping and mating analysis suggested that both MC-RGS5 and

MV-RGS5 mice were viable and fertile without visible developmental defects. Gross morphology of embryos from both transgenic mice did not exhibit noticeable phenotypes such as growth retardation and cardiovascular defect when compared with non-transgenic siblings. However, the majority of offspring from mating of MC-RGS5 females and C57BL6 males died within 1~2 days after birth, associated with a reduced level or the total absence of milk in their stomachs, even though MC-RGS5 female transgenic mice demonstrated normal maternal behavior. MC-RGS5 females built a typical nest and quickly retrieved offspring that moved outside of the nest. In contrast, the postnatal lethality was not observed in pups from mating of MC-RGS5 male and C57BL6 female. This phenotype mimics that of oxytocin null mice (Nishimori, Young et al. 1996). Since it is known that RGS5 negatively regulates oxytocin receptor, one of Gq-protein coupled receptors, the above-mentioned defect of MC-RGS5 may result from the failure of oxytocin-induced mammary gland and uterine smooth muscle contraction. Taken together, RGS5 may play a role in controlling contraction in various smooth muscle-containing tissues. These transgenic models may be used as a valuable tool to characterize the homeostasis of RGS5 turnover in contractile pathway and to determine *in vivo* function of posttranslational modification of N-terminal degradation determinant, Cys-2, of RGS5 in vascular signaling and development.

3.3 METHODS

Construction of MC-RGS5 and MV-RGS5 Transgenic mice. The wild type (MC) murine RGS5 cDNA (genebank accession no. NM_009063) and mutant (MV) RGS5 cDNA were released with BamHI, and ligated into the BamHI site of a plasmid containing the 481-bp murine SM22alpha (Transgelin, -441 to 41 relative to transcription start) promoter provided by Dr. Andrea Ekhart (Thomas Jefferson University, Philadelphia, PA) (genebank accession no. U36589) (Eckhart, Ozaki et al. 2002). The resulting recombinant plasmids, SM22α-MC-RGS5 or SM22a-MV-RGS5, were confirmed by restriction enzyme mapping and nucleotide sequencing. A linear 1.9 kb DNA fragment containing the SM22α promoter, the complete murine MC-RGS5 or MV-RGS5 cDNA ORF, and a simian virus 40 (SV40) intron and polyadenylylation signal was released by digestion with XhoI and SacII (**Fig.13**). This fragment was microinjected into male pronuclei of fertilized C57BL6 mouse oocytes and implanted into pseudopregnant females by Transgenic and Gene Targeting Core Facility in University of Pittsburgh. Three-week-old mouse pups were screened for presence of the transgene by Southern analysis. From second generation, nested PCR was performed for genotyping.

Southern Blot. Random integration of transgene into mouse genome was accessed by Southern blot analysis from tail genomic DNAs of three-week-old mice. Tail genomic DNAs (10g) were digested with SalI, electrophoresed on a 1% agarose gel, transfered to Nytran membrane (Wattman), and hybridized with ^{32}P-labeled 800-bp BamHI–SacII fragment of SV40 viral DNA. Probe was labeled using [^{32}P]dCTP by Ready-To-Go DNA Labelling Beads (Amersham) and radiolabeled probe was purified by ProbeQuant G-50 Micro Columns

(Amersham). The membrane was prehybridized in ExpressHyb Solution (Clontech) and radiolabeled DNA probe with 100mg/ml salmon sperm DNA was added to the filter at 60°C for 4 hours. Membranes were washed several times and exposed to Kodak Biomax MS film with an intensifying screen. Approximate copy numbers were estimated by comparison of signal intensity with that of copy numbers of transgene.

Genotyping. Genomic DNA from embryo yolk sacs or mouse tails was analyzed by nested PCR amplification using two primer pair sets (**Fig.13**). The first-round PCR primers (outer primer pairs) were designed to have a forward primer on 5' upstream of SM22α promoter and a reverse primer on poly A signal, amplifying 1,295-bp and their sequences are SM5 (5'-CAGTCAAGACTAGTTCCCACCAACTCG-3') and Poly3 (5'-CTAGATGGCATTTCTTCTGAGCAAAACAG-3'). The second-round PCR primers (inner primer pairs) were designed to detect the inner sequence of the first-round PCR product, amplifying 1,184-bp and their sequences are SM6 (5'-CAGGTTCCTTTGTCGGGCCAAACTCTAG-3') and Poly4 (5'-GGCATTCCACCACTGCTCCCATTCATC-3').

Western Blot. Different tissues including aorta, heart, uterus, liver, and brain from two-month-old mice were dissected in cold PBS and homogenized in RIPA lysis buffer (150mM Sodium Chloride, 1% NP-40, 0.5% Sodium deoxycholate, 0.1% SDS, 50mM Tris, pH 8.0) containing a protease inhibitor cocktail (Sigma). Protein concentration was determined using the BCA protein assay (Pierce, Rockford, Ill.) with bovine serum albumin as a standard. Approximately 30ug of total protein extract from each tissue was subjected to electrophoresis

and transfered to polybvinylidene fluoride (PVDF) membrane, and stained with anti-RGS5 antibody (gift of Dr. Jian Li, Havard University), followed by re-staining with anti-actin antibody (Sigma) as a loading control.

Cell Culture and Transfection. A7r5 cells, rat aortic smooth muscle cells (ATCC), were maintained in DMEM supplemented with 10% FBS and 100U/ml penicillin/streptomycin. For transfection, cells were plated at 3 x 10^4 cells/well in 12-well plate and transfected with 1ug of plasmid using Lipofectamine LTX by manufacturer's protocol. Cells were maintained for 44 hours, treated with 5μM of MG132 for 4 hours, and harvested.

Immunohistochemistry. Thoracic aorta was dissected in cold PBS and fixed overnight at 4°C in 4% paraformaldehyde (Fisher Scientific) in PBS. Samples were stored in 70% ethanol at 4°C after several washing with PBS. For histological analysis, samples were dehydrated in serial ethanol, cleared in histosol (National Diagnostics), paraffin-embedded, and sectioned transversely at 5μm. Sections were antigen-retrieved by heating in Tris-EDTA (pH. 9.0) for 20 min using a microwave oven, and blocked in PBST (0.2% Triton X-100 in PBS) containing 1% BSA for 1.5 hrs, and incubated with primary antibody (rabbit anti-RGS5 antibody (1:400), a gift from Dr. Li in Harvard University; mouse anti-α smooth muscle actin (1:400), Sigma) in PBS with 0.5% BSA overnight, followed by secondary antibody (Alexa 555-conjugated anti-rabbit IgG; Alexa 48- conjugated anti-mouse IgG2a, Invitrogen) in PBS for 1 hr. Sections were counterstained with 4'6'-diamidino-2-phenylindole (DAPI, Vector Laboratories) to visualize the nuclei.

3.4 RESULTS

To investigate the role of RGS5 proteolysis in vascular smooth muscle cells, MC-RGS5 and MV-RGS5 transgenic mice carrying the construct shown in **Figure 13** were produced as described in *Methods*. I used the mouse SM22alpha promoter, which has been well characterized to target transgene expression to arterial but not venous or visceral smooth muscle cells (Eckhart, Ozaki et al. 2002; Keys, Zhou et al. 2005). A schematic diagram of the transgene construct is presented in Fig. 13. Briefly, the SM22α promoter (-441 to +41) was fused to the cDNA of mouse RGS5 (MC-RGS5 or MV-RGS5) and the SV40 poly A signal sequence by conventional cloning. MV-RGS5 cDNA was simply generated by replacing Cys-2 encoded-TGT with Val-encoded GTG. Southern blot analysis of tail genomic DNA identified one potential MC-RGS5 and one potential MV-RGS5 transgenic founders (**Figure 14**). However, this analysis was not sensitive enough to detect 1 and 5 copies of transgene. Further analysis using nested PCR primer sets revealed two more MC-RGS5 male founders and another putative MV-RGS5 founder (**Figure 15**). Five of the founder animals were viable and fertile, but only three of them (one MC-RGS5 female, one MV-RGS5 female, and one MV-RGS5 male) exhibited germline transmission of the transgene to subsequent progeny.

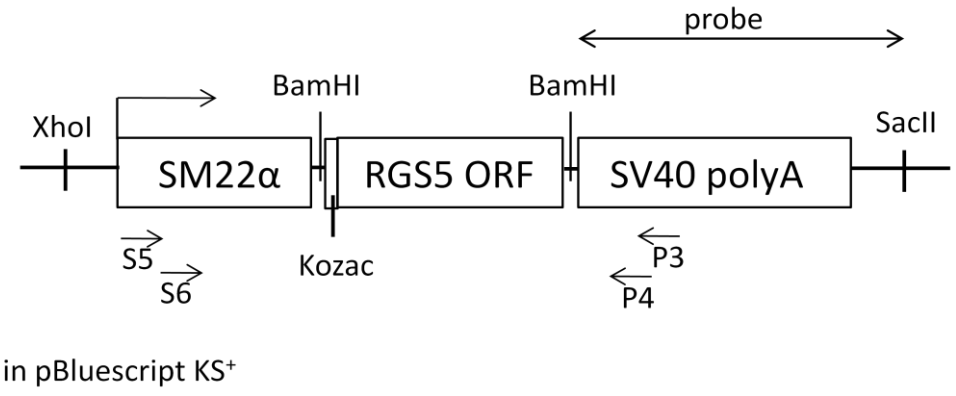

Figure 13. Schematic diagram of RGS5 transgenic construct. Full-length cDNA of RGS5 (MC-RGS5 and MV-RGS5) including kozac sequence and the SV40 large T antigen polyadenylation signal sequence (SV40 polyA) were inserted into a modified pBluescript KS^+ vector under the SM22alpha promoter (-441 to +41). To generate MV-RGS5 TG mice, TGT encoding second Cys amino acid was replaced by GTG encoding Val. Restriction sites for excision of the construct from the cloning vector (XhoI/SacII) and for generation of radiolabeled probe (BamHI/SacII) are indicated with solid line. The primers for nested PCR are indicated as arrows labeled with S5 (SM5), S6 (SM6), P3 (poly3), and P4 (poly4).

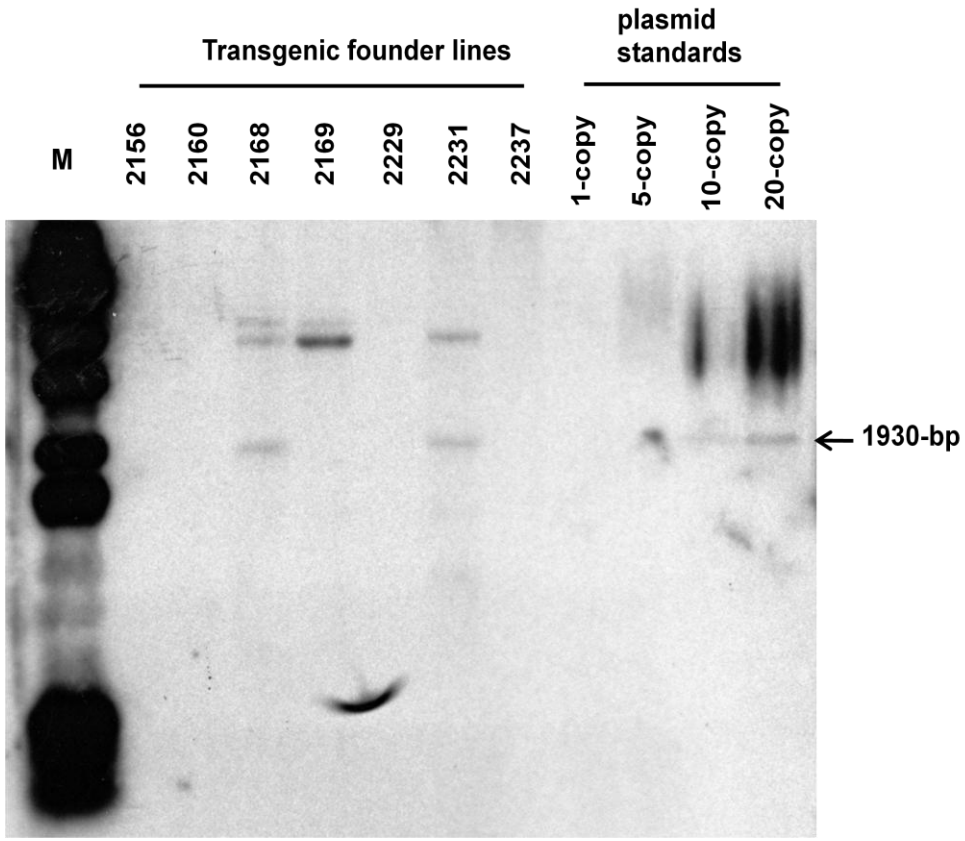

Figure 14. Southern blot analysis to identify founder transgenic mice. Tail DNA was digested with Sal I to generate a 800-bp fragment containing the SV40 polyadenylation sequence from the transgene (see ***Fig.13***). 10 μg of digested genomic DNA was resolved by gel electrophoresis and transferred to Nytran, and the membrane was incubated with ^{32}P-labeled probe. The copy number standards were produced from transgenic construct plasmids. M, DNA marker.

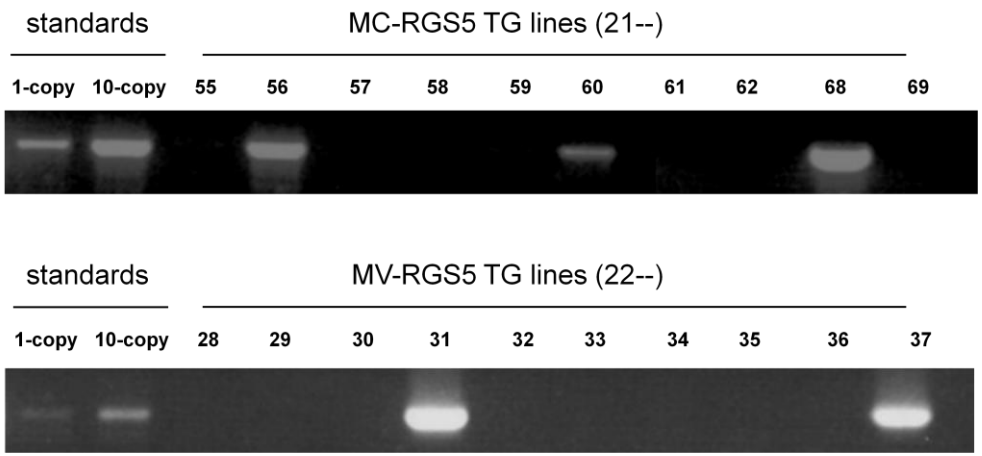

Figure 15. Genotyping of F0 generation of RGS5 TG mice. Nested PCR was performed to detect RGS5 transgene using genomic DNA from mouse tails as a template for PCR genotype screening. The transgenic plasmid was loaded to estimate approximate copy number of RGS5 transgene expression.

To analyze RGS5 transgenic expression, transgenic tissues including aorta, heart, uterus, liver, and brain from two-month-old MC-RGS5 and MV-RGS5 mice were dissected and lysed followed by western blotting using anti-RGS5 antibody (**Figure 16**). Consistent with the previous northern blot analysis showing that RGS5 mRNA is abundantly expressed in heart, lung, and intestine and at low levels in brain, liver, and placenta (Seki, Sugano et al. 1998), high levels of endogenous RGS proteins were detected in heart and aorta of NTG mice, whereas relatively lower amounts of RGS proteins were detected in liver and brain and, more significantly, uterus. This suggests that endogenous RGS5 is widely distributed in various smooth muscle-containing tissues. Immunoblotting of transgenic tissues revealed that MC-RGS5 TG mice contain a higher level of RGS5 compared to that in control mice (**Figure 16**). Consistent with the finding that RGS5 Cys-2 is a degradation determinant, MV-RGS5 tissues showed an even higher level of RGS5 compared to MC-RGS5 mice (**Figure 16**). These results together suggest that RGS5 in these transgenic mice undergoes at least in part N-end rule degradation based on Cys-2 as a degron.

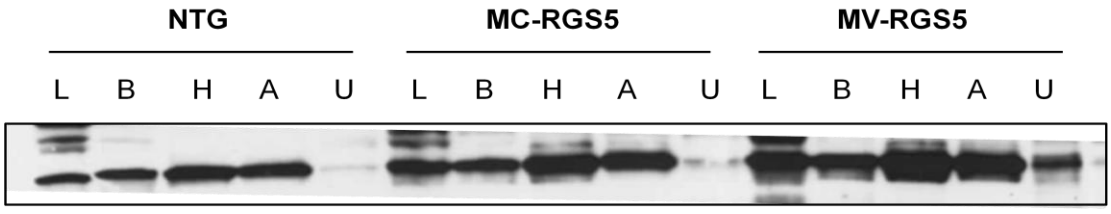

Figure 16. Tissue distribution of RGS5 protein. RGS5 protein levels in different tissues of adult RGS5 transgenic mice and non-transgenic mice (NTG) were determined by Western blotting. L, Liver; B, brain; H, heart; A, aorta; U, uterus.

To confirm VSMC-specific transgenic expression, thoracic aorta from two types of transgenic mice were isolated and immunostained with anti-RGS5 antibody, followed by staining of the cross sections for α-smooth muscle actin (αSMA), a marker of VSMC (**Figure 17**). NTG aorta demonstrated that endogenous RGS5 is expressed at basal level, whereas the aorta of both MC-RGS5 and MV-RGS5 exhibited higher level of RGS5 expression in VSMC, displaying co-localized expression with αSMA.

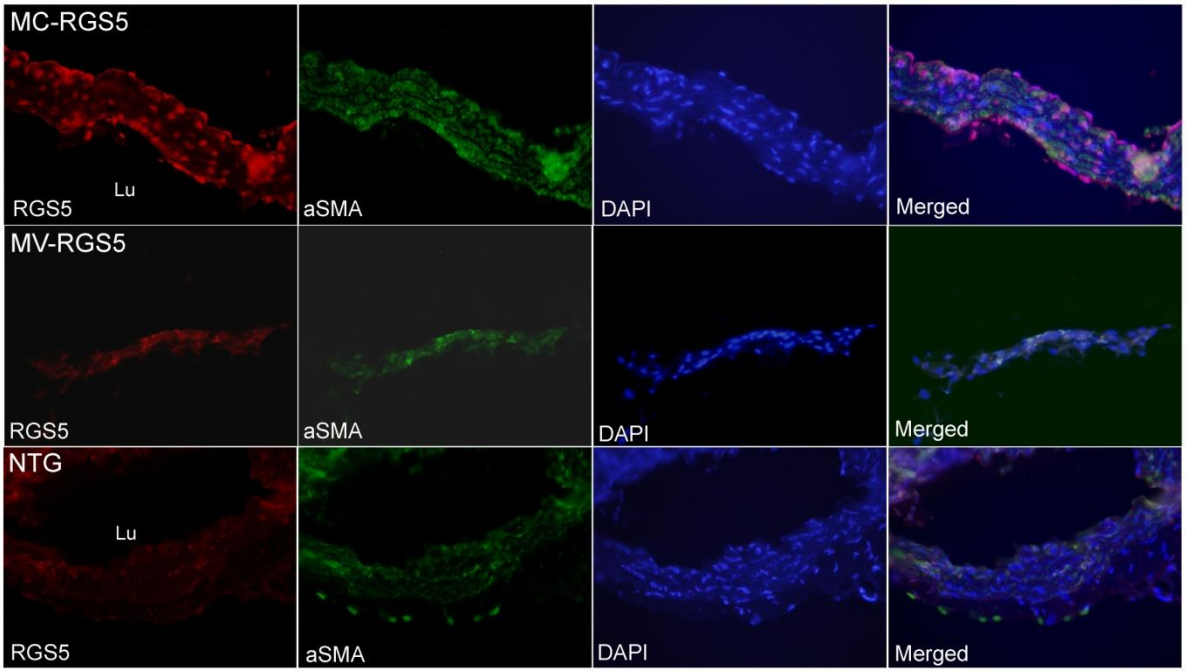

Figure 17. RGS5 expression in the aorta of MC-RGS5, MV-RGS5, and NTG mice. Transverse section of thoracic aorta were stained for RGS5 (red), α-SMA (green) and nucleus (blue) as indicated above. Lu, Lumen.

To determine the role of Cys-2 as an N-terminal degradation determinant in A7r5, vascular smooth muscle cells (VSMC), RGS5 transgenic constructs overexpressing either MC-RGS5 or MV-RGS5 from SM22α promoter were transiently transfected, followed by immunoblotting with anti-RGS5 antibody. The EGFP plasmid from SM22α promoter was additionally constructed to confirm the VSMC-specific promoter activity in VSMC and to optimize the transfection efficiency by visualized EGFP signal (**Figure 18B**). Transient EGFP expression indicated that up to 30% of VSMC can be transfected in a dose-dependent manner. For RGS5 constructs, as expected, wild-type MC-RGS5 (short-lived) was rapidly degraded in VSMC, whereas the degradation of mutant MV-RGS5 (long-lived) was significantly abolished (**Figure 18C**), implicating that RGS5 proteolysis is governed by N-end rule pathway.

Although both MC-RGS5 and MV-RGS5 transgenic mice were fertile, newborn pups from MC-RGS5 female were found dead or cannibalized by their mother, associated with a reduced level or the total absence of milk in their stomachs, whereas MV-RGS5 female did not display this phenotype. **Table 2** shows that 6 out of 7 deliveries (21 out of 38 mice) in MC-RGS5 female failed, resulting in neonatal lethality. However, this impaired delivery was recovered after 2~3 rounds of labor. The ratio of transgenic mice in the offsprings from MC-RGS5 female (27%) with smaller litter size is lower than that in the offsprings from MC-RGS5 male (51%) (**Table 2**). The offsprings from female and male MV-RGS5 TG mice were recovered at Mendelian ratios. The transgenic ratios of the offsprings were determined to be 67% and 41%, respectively. These results together suggest partial embryonic lethality may be caused by suboptimal conditions of MC-RGS5 female during pregnancy.

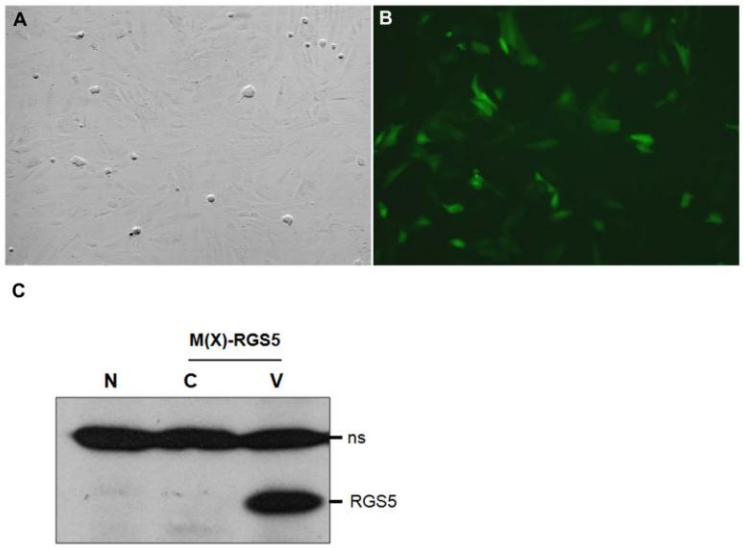

Figure 18. Establishing the expression of transient transfection of mouse RGS5 into A7r5 cells. (A) and (B) show fluorescence microscopy images 48 h after transient transfection of rat aortic smooth muscle cells A7r5 with the EGFP construct under SM22α promoter. Phase contrast (A) and the corresponding fluorescence (B) image show that GFP expression is seen throughout the cell cytosol. Magnification ×100 (C) Western blotting of transfected cell lysates for MC-RGS5 and MV-RGS5 constructs. The non-specific band (ns) shows equal amount of loading in each sample.

Table 2. The offsprings phenotype from MC-RGS5 and MV-RGS5 TG mice.

MC-RGS5 offsprings						
Paternal	Maternal	n	# of lethality	# of lethal mice	Litter size	% of TG
C57BL6	MC-RGS5	7	6	21/38	5.5	27
MC-RGS5	C57BL6	5	0	0/35	7	51
MV-RGS5 offsprings						
C57BL6	MV-RGS5	3	0	0/24	8	67
MV-RGS5	C57BL6	4	0	0/27	6.8	41

To examine the physiological function of RGS5, I harvested embryos from MC-RGS5 and MV-RGS5 TG mice at E16.5 and E14.5, respectively (**Figure 19**). Given that RGS5 is one of ATE1 substrates and that ATE1 null mice revealed severe cardiovascular defect from E12.5, I expected that RGS5 TG mice may have similar cardiovascular phenotype or at least milder phenotype. However, both MC-RGS5 and MV-RGS5 TG embryos displayed no obvious developmental defects and the vasculature appeared to develop normally in comparison to wild-type siblings. Therefore, the overexpression of RGS5 in smooth muscle cells does not induce noticeable developmental defects in embryos.

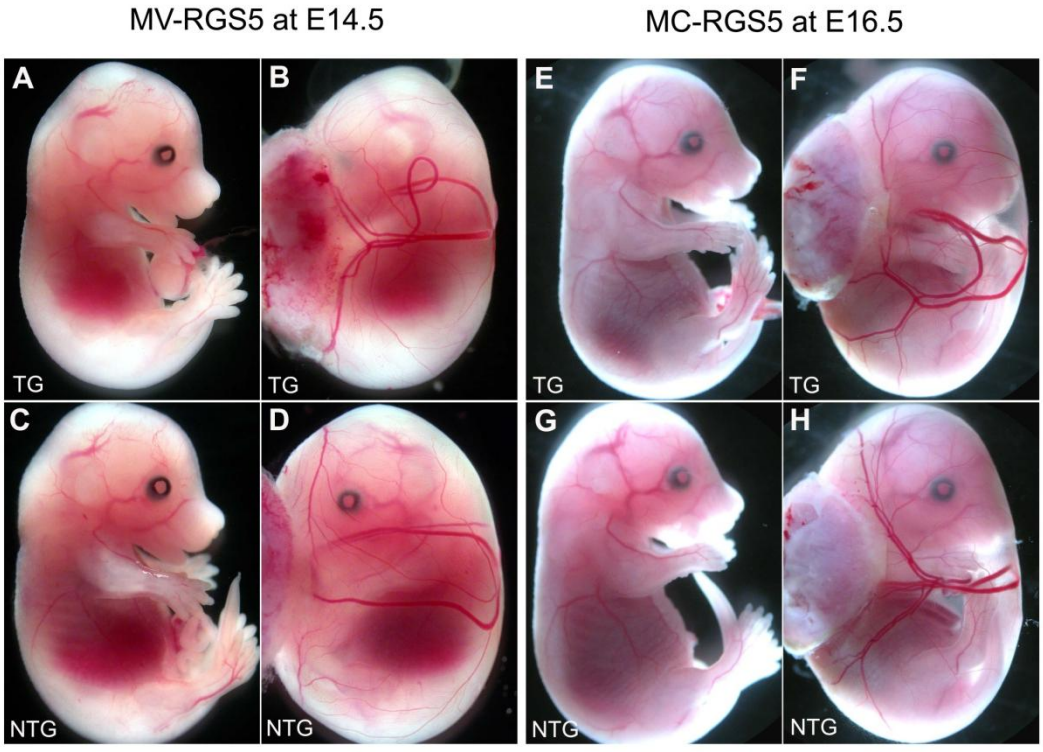

Figure 19. Gross morphology of embryos and yolk sacs of MV-RGS5 at E14.5 (A~D) and MC-RGS5 at E16.5 (E~H).

3.5 DISCUSSION

The most obvious phenotype from RGS5 TG mice is the lethality of offspring during or after labor from MC-RGS5 TG females. It is commonly observed that first time mothers and very young females cannibalize their litters, but as they become experienced and mature, they raise their litters successfully. However, this is not the case in RGS5 TG mice, because the same phenotype was observed in 2~3 rounds of labor for each of MC-RGS5 TG females. Literature search revealed that this phenotype is very similar to that observed with oxytocin null mice (Nishimori, Young et al. 1996). It is notable that oxytocin receptor is one of Gq-coupled GPCRs. During delivery, oxytocin binds Gq-coupled GPCR and induces the contraction of uterine smooth muscle and mammary smooth muscle to help laboring and produce milking. Therefore, the phenotype observed with MC-RGS5 TG mice appears to be related with the failure of oxytocin-activated smooth muscle contraction due to inhibitory effect of RGS5 overexpression. In addition, the fact that this phenotype is only found in MC-RGS5 female, not in MV-RGS5 female, suggests that MV-RGS5 may not be functional *in vivo*. A recent study has shown that RGS2 and RGS5 were abundantly expressed at various stages of pregnancy (non-pregnant, preterm, term non-labouring, and term laboring) in human (Ladds, Zervou et al. 2009). The co-immunoprecipitation assay showed that RGS2 and RGS5 interact with the oxytocin receptor, further suggesting that functional MC-RGS5 negatively regulates the oxytocin receptor signaling.

RGS5-deficient mice generated by two independent groups have been shown to be hypotensive relative to wild-type controls (Cho, Park et al. 2008; Nisancioglu, Mahoney et al. 2008). This result is apparently unexpected because, given the function of RGS5 as a GTPase

activating protein (GAP) in Gαq- and Gαi-mediated cardiovascular signaling, it has been expected that RGS5 inactivation would cause hypertension rather than hypotension. One feasible explanation is that the functionally related RGS2 and RGS4 may compensate the loss of RGS5, which lowers BP. Together with RGS5, RGS2, a member of RGS4 subfamily, is emerging as a key regulator of the blood pressure (BP). RGS2 is a potent negative regulator of Gαq, which mediates the action of most physiological vasoconstrictors, including norepinephrine, angiotensin II, endothelin-1, and thrombin (Heximer, Knutsen et al. 2003). Mice lacking RGS2 are hypertensive due to the increased vascular tone in the BP homeostasis (Heximer, Knutsen et al. 2003; Gu, Cifelli et al. 2009). These results suggest that RGS5 together with RGS2 and RGS4 participate in the regulation of BP homeostasis. The possible consequence of perturbation of RGS5 turnover in RGS5 TG mice is dampened vascular Gq signaling involved in controlling BP. I anticipate that the accumulation of RGS5 in VSMC results in hypotension.

Another interesting study using RGS5 TG mice is to characterize the physiological importance of oxidation of Cys-2 of RGS5 in VSMC. Given that NADPH oxidase is a major generator of ROS in VSMC among various ROS sources including NADPH oxidases, xanthine oxidase, mitochondrial electron transport system, cytochrom p450, nitric oxide synthase (NOS) (Landmesser, Cai et al. 2002; Clempus and Griendling 2006), the reactive oxygen species (ROS) generated from NADPH oxidase may play a role in RGS5 oxidation in VSMC. It has been shown that loss of p47phox, a critical subunit of NADPH oxidase, resulted in impaired ROS production when cultured VSMC were stimulated by angiotensin II or PDGF-ββ. The loss of p47phox resulted in lower BP in mice. These results suggest that NADPH oxidase-generated ROS is involves in angiotensin II-induced BP homeostasis (Landmesser, Cai et al. 2002). NADPH oxidase-produced ROS induces calcium-independent activation of the Rho-GTP

pathway, in which Rho-GTP-activated kinase inhibits MLC phosphatase (MLCP) and, thus, accelerates phosphorylation of myosin light chain (MLC), leading to smooth muscle contraction (Jin, Ying et al. 2004). Taken together with these results, the oxidation of RGS5 Cys-2 via NADPH oxidase-produced ROS may negatively regulate Gq agonists-induced vascular signaling, which in turn modulates vascular smooth muscle contraction and BP controlling (Clempus and Griendling 2006). This transgenic model will be a useful tool to determine whether the steady state level of RGS5 in vascular smooth muscle cells (VSMC) of blood vessels as well as uterine SMC is regulated by the N-end rule pathway through its posttranslational modifications such as oxidation, arginylation, ubiquitination and degradation. Successful results will provide a molecular basis in homeostasis of cardiovascular Gq signaling.

BIBLIOGRAPHY

Adams, J. W., A. L. Pagel, et al. (2000). "Cardiomyocyte apoptosis induced by Galphaq signaling is mediated by permeability transition pore formation and activation of the mitochondrial death pathway." Circ Res **87**(12): 1180-7.

An, J. Y., J. W. Seo, et al. (2006). "Impaired neurogenesis and cardiovascular development in mice lacking the E3 ubiquitin ligases UBR1 and UBR2 of the N-end rule pathway." Proc Natl Acad Sci U S A **103**(16): 6212-7.

Balogh, S. A., Y. T. Kwon, et al. (2000). "Varying intertrial interval reveals temporally defined memory deficits and enhancements in NTAN1-deficient mice." Learn Mem **7**(5): 279-86.

Berger, M., G. Bergers, et al. (2005). "Regulator of G-protein signaling-5 induction in pericytes coincides with active vessel remodeling during neovascularization." Blood **105**(3): 1094-101.

Blizard, D. A. and R. Welty (1971). "Cardiac activity in the mouse: strain differences." J Comp Physiol Psychol **77**(2): 337-44.

Bondjers, C., M. Kalen, et al. (2003). "Transcription profiling of platelet-derived growth factor-B-deficient mouse embryos identifies RGS5 as a novel marker for pericytes and vascular smooth muscle cells." Am J Pathol **162**(3): 721-9.

Brower, C. S. and A. Varshavsky (2009). "Ablation of arginylation in the mouse N-end rule pathway: loss of fat, higher metabolic rate, damaged spermatogenesis, and neurological perturbations." PLoS One **4**(11): e7757.

Callaghan, M. J., A. J. Russell, et al. (1998). "Identification of a human HECT family protein with homology to the Drosophila tumor suppressor gene hyperplastic discs." Oncogene **17**(26): 3479-91.

Cho, H., T. Kozasa, et al. (2003). "Pericyte-specific expression of Rgs5: implications for PDGF and EDG receptor signaling during vascular maturation." FASEB J **17**(3): 440-2.

Cho, H., C. Park, et al. (2008). "Rgs5 targeting leads to chronic low blood pressure and a lean body habitus." Mol Cell Biol **28**(8): 2590-7.

Clempus, R. E. and K. K. Griendling (2006). "Reactive oxygen species signaling in vascular smooth muscle cells." Cardiovasc Res **71**(2): 216-25.

Creazzo, T. L., R. E. Godt, et al. (1998). "Role of cardiac neural crest cells in cardiovascular development." Annu Rev Physiol **60**: 267-86.

D'Angelo, D. D., Y. Sakata, et al. (1997). "Transgenic Galphaq overexpression induces cardiac contractile failure in mice." Proc Natl Acad Sci U S A **94**(15): 8121-6.

de Groot, R. J., T. Rumenapf, et al. (1991). "Sindbis virus RNA polymerase is degraded by the N-end rule pathway." Proc Natl Acad Sci U S A **88**(20): 8967-71.

DeMasi, J., K. W. Huh, et al. (2005). "Bovine papillomavirus E7 transformation function correlates with cellular p600 protein binding." Proc Natl Acad Sci U S A **102**(32): 11486-91.

Ditzel, M., R. Wilson, et al. (2003). "Degradation of DIAP1 by the N-end rule pathway is essential for regulating apoptosis." Nat Cell Biol **5**(5): 467-73.

Eckhart, A. D., T. Ozaki, et al. (2002). "Vascular-targeted overexpression of G protein-coupled receptor kinase-2 in transgenic mice attenuates beta-adrenergic receptor signaling and increases resting blood pressure." Mol Pharmacol **61**(4): 749-58.

Furuya, M., M. Nishiyama, et al. (2004). "Expression of regulator of G protein signalling protein 5 (RGS5) in the tumour vasculature of human renal cell carcinoma." J Pathol **203**(1): 551-8.

Grigoryev, S., A. E. Stewart, et al. (1996). "A mouse amidase specific for N-terminal asparagine. The gene, the enzyme, and their function in the N-end rule pathway." J Biol Chem **271**(45): 28521-32.

Gu, S., C. Cifelli, et al. (2009). "RGS proteins: identifying new GAPs in the understanding of blood pressure regulation and cardiovascular function." Clin Sci (Lond) **116**(5): 391-9.

Hamzah, J., M. Jugold, et al. (2008). "Vascular normalization in Rgs5-deficient tumours promotes immune destruction." Nature **453**(7193): 410-4.

Henderson, M. J., M. A. Munoz, et al. (2006). "EDD mediates DNA damage-induced activation of CHK2." J Biol Chem **281**(52): 39990-40000.

Hershko, A. and A. Ciechanover (1998). "The ubiquitin system." Annu Rev Biochem **67**: 425-79.

Heximer, S. P., R. H. Knutsen, et al. (2003). "Hypertension and prolonged vasoconstrictor signaling in RGS2-deficient mice." J Clin Invest **111**(8): 1259.

Heydemann, A., J. M. Huber, et al. (2005). "Genetic background influences muscular dystrophy." Neuromuscul Disord **15**(9-10): 601-9.

Hoit, B. D., S. Kiatchoosakun, et al. (2002). "Naturally occurring variation in cardiovascular traits among inbred mouse strains." Genomics **79**(5): 679-85.

Hu, R. G., C. S. Brower, et al. (2006). "Arginyltransferase, its specificity, putative substrates, bidirectional promoter, and splicing-derived isoforms." J Biol Chem **281**(43): 32559-73.

Hu, R. G., J. Sheng, et al. (2005). "The N-end rule pathway as a nitric oxide sensor controlling the levels of multiple regulators." Nature **437**(7061): 981-6.

Huh, K. W., J. DeMasi, et al. (2005). "Association of the human papillomavirus type 16 E7 oncoprotein with the 600-kDa retinoblastoma protein-associated factor, p600." Proc Natl Acad Sci U S A **102**(32): 11492-7.

Jaber, M., W. J. Koch, et al. (1996). "Essential role of beta-adrenergic receptor kinase 1 in cardiac development and function." Proc Natl Acad Sci U S A **93**(23): 12974-9.

Jackson, I. J. and C. M. Abbott (2000). Mouse genetics and transgenics : a practical approach. Oxford ; New York, Oxford University Press.

Jin, L., Z. Ying, et al. (2004). "Activation of Rho/Rho kinase signaling pathway by reactive oxygen species in rat aorta." Am J Physiol Heart Circ Physiol **287**(4): H1495-500.

Kaji, H., G. D. Novelli, et al. (1963). "A Soluble Amino Acid-Incorporating System from Rat Liver." Biochim Biophys Acta **76**: 474-7.

Kardestuncer, T., H. Wu, et al. (1998). "Cardiac myocytes express mRNA for ten RGS proteins: changes in RGS mRNA expression in ventricular myocytes and cultured atria." FEBS Lett **438**(3): 285-8.

Keys, J. R., R. H. Zhou, et al. (2005). "Vascular smooth muscle overexpression of G protein-coupled receptor kinase 5 elevates blood pressure, which segregates with sex and is dependent on Gi-mediated signaling." Circulation **112**(8): 1145-53.

Kirsch, T., M. Wellner, et al. (2001). "Altered gene expression in cerebral capillaries of stroke-prone spontaneously hypertensive rats." Brain Res **910**(1-2): 106-15.

Kwon, Y. T., S. A. Balogh, et al. (2000). "Altered activity, social behavior, and spatial memory in mice lacking the NTAN1p amidase and the asparagine branch of the N-end rule pathway." Mol Cell Biol **20**(11): 4135-48.

Kwon, Y. T., A. S. Kashina, et al. (2002). "An essential role of N-terminal arginylation in cardiovascular development." Science **297**(5578): 96-9.

Kwon, Y. T., A. S. Kashina, et al. (1999). "Alternative splicing results in differential expression, activity, and localization of the two forms of arginyl-tRNA-protein transferase, a component of the N-end rule pathway." Mol Cell Biol **19**(1): 182-93.

Kwon, Y. T., F. Levy, et al. (1999). "Bivalent inhibitor of the N-end rule pathway." J Biol Chem **274**(25): 18135-9.

Kwon, Y. T., Y. Reiss, et al. (1998). "The mouse and human genes encoding the recognition component of the N-end rule pathway." Proc Natl Acad Sci U S A **95**(14): 7898-903.

Kwon, Y. T., Z. Xia, et al. (2003). "Female lethality and apoptosis of spermatocytes in mice lacking the UBR2 ubiquitin ligase of the N-end rule pathway." Mol Cell Biol **23**(22): 8255-71.

Kwon, Y. T., Z. Xia, et al. (2001). "Construction and analysis of mouse strains lacking the ubiquitin ligase UBR1 (E3alpha) of the N-end rule pathway." Mol Cell Biol **21**(23): 8007-21.

Ladds, G., S. Zervou, et al. (2009). "Regulators of G protein signalling proteins in the human myometrium." Eur J Pharmacol **610**(1-3): 23-8.

Landmesser, U., H. Cai, et al. (2002). "Role of p47(phox) in vascular oxidative stress and hypertension caused by angiotensin II." Hypertension **40**(4): 511-5.

Lee, M. J., T. Tasaki, et al. (2005). "RGS4 and RGS5 are in vivo substrates of the N-end rule pathway." Proc Natl Acad Sci U S A **102**(42): 15030-5.

Lippert, E., D. L. Yowe, et al. (2003). "Role of regulator of G protein signaling 16 in inflammation-induced T lymphocyte migration and activation." J Immunol **171**(3): 1542-55.

Mende, U., A. Kagen, et al. (1998). "Transient cardiac expression of constitutively active Galphaq leads to hypertrophy and dilated cardiomyopathy by calcineurin-dependent and independent pathways." Proc Natl Acad Sci U S A **95**(23): 13893-8.

Michele, D. E., C. A. Gomez, et al. (2002). "Cardiac dysfunction in hypertrophic cardiomyopathy mutant tropomyosin mice is transgene-dependent, hypertrophy-independent, and improved by beta-blockade." Circ Res **91**(3): 255-62.

Mittmann, C., C. H. Chung, et al. (2002). "Expression of ten RGS proteins in human myocardium: functional characterization of an upregulation of RGS4 in heart failure." Cardiovasc Res **55**(4): 778-86.

Nisancioglu, M. H., W. M. Mahoney, Jr., et al. (2008). "Generation and characterization of rgs5 mutant mice." Mol Cell Biol **28**(7): 2324-31.

Nishimori, K., L. J. Young, et al. (1996). "Oxytocin is required for nursing but is not essential for parturition or reproductive behavior." Proc Natl Acad Sci U S A **93**(21): 11699-704.

Owen, V. J., P. B. Burton, et al. (2001). "Expression of RGS3, RGS4 and Gi alpha 2 in acutely failing donor hearts and end-stage heart failure." Eur Heart J **22**(12): 1015-20.

Patten, M., J. Bunemann, et al. (2002). "Endotoxin induces desensitization of cardiac endothelin-1 receptor signaling by increased expression of RGS4 and RGS16." Cardiovasc Res **53**(1): 156-64.

Prabhakar, R., G. P. Boivin, et al. (2001). "A familial hypertrophic cardiomyopathy alpha-tropomyosin mutation causes severe cardiac hypertrophy and death in mice." J Mol Cell Cardiol **33**(10): 1815-28.

Rai, R. and A. Kashina (2005). "Identification of mammalian arginyltransferases that modify a specific subset of protein substrates." Proc Natl Acad Sci U S A **102**(29): 10123-8.

Rao, H., F. Uhlmann, et al. (2001). "Degradation of a cohesin subunit by the N-end rule pathway is essential for chromosome stability." Nature **410**(6831): 955-9.

Rogers, J. H., P. Tamirisa, et al. (1999). "RGS4 causes increased mortality and reduced cardiac hypertrophy in response to pressure overload." J Clin Invest **104**(5): 567-76.

Rogers, J. H., A. Tsirka, et al. (2001). "RGS4 reduces contractile dysfunction and hypertrophic gene induction in Galpha q overexpressing mice." J Mol Cell Cardiol **33**(2): 209-18.

Schlager, G. (1966). "Systolic blood pressure in eight inbred strains of mice." Nature **212**(5061): 519-20.

Seki, N., S. Sugano, et al. (1998). "Isolation, tissue expression, and chromosomal assignment of human RGS5, a novel G-protein signaling regulator gene." J Hum Genet **43**(3): 202-5.

Sriram, S. M., R. Banerjee, et al. (2009). "Multivalency-assisted control of intracellular signaling pathways: application for ubiquitin- dependent N-end rule pathway." Chem Biol **16**(2): 121-31.

Stewart, A. E., S. M. Arfin, et al. (1995). "The sequence of porcine protein NH2-terminal asparagine amidohydrolase. A new component of the N-end Rule pathway." J Biol Chem **270**(1): 25-8.

Tamirisa, P., K. J. Blumer, et al. (1999). "RGS4 inhibits G-protein signaling in cardiomyocytes." Circulation **99**(3): 441-7.

Tasaki, T. and Y. T. Kwon (2007). "The mammalian N-end rule pathway: new insights into its components and physiological roles." Trends Biochem Sci **32**(11): 520-8.

Tasaki, T., L. C. Mulder, et al. (2005). "A family of mammalian E3 ubiquitin ligases that contain the UBR box motif and recognize N-degrons." Mol Cell Biol **25**(16): 7120-36.

Tominaga, K., J. Matsuda, et al. (2004). "Genetic background markedly influences vulnerability of the hippocampal neuronal organization in the "twitcher" mouse model of globoid cell leukodystrophy." J Neurosci Res **77**(4): 507-16.

Wieland, T. and C. Mittmann (2003). "Regulators of G-protein signalling: multifunctional proteins with impact on signalling in the cardiovascular system." Pharmacol Ther **97**(2): 95-115.

Zhang, S., N. Watson, et al. (1998). "RGS3 and RGS4 are GTPase activating proteins in the heart." J Mol Cell Cardiol **30**(2): 269-76.

Zhou, J., K. Moroi, et al. (2001). "Characterization of RGS5 in regulation of G protein-coupled receptor signaling." Life Sci **68**(13): 1457-69.